



UNIVERSITÀ  
DEGLI STUDI  
FIRENZE

## FLORE

# Repository istituzionale dell'Università degli Studi di Firenze

### **Modifications on the Amino-3,5-dicyanopyridine Core To Obtain Multifaceted Adenosine Receptor Ligands with Antineuropathic**

Questa è la Versione finale referata (Post print/Accepted manuscript) della seguente pubblicazione:

*Original Citation:*

Modifications on the Amino-3,5-dicyanopyridine Core To Obtain Multifaceted Adenosine Receptor Ligands with Antineuropathic Activity / Betti, Marco; Catarzi, Daniela; Varano, Flavia; Falsini, Matteo; Varani, Katia; Vincenzi, Fabrizio; Pasquini, Silvia; di Cesare Mannelli, Lorenzo; Ghelardini, Carla; Lucarini, Elena; Dal Ben, Diego; Spinaci, Andrea; Bartolucci, Gian Luca; Menicatti, Marta; Colotta, Vittoria. - In: JOURNAL OF

*Availability:*

The webpage <https://hdl.handle.net/2158/1170035> of the repository was last updated on 2024-04-22T13:19:13Z

*Published version:*

DOI: 10.1021/acs.jmedchem.9b00106

*Terms of use:*

Open Access

La pubblicazione è resa disponibile sotto le norme e i termini della licenza di deposito, secondo quanto stabilito dalla Policy per l'accesso aperto dell'Università degli Studi di Firenze (<https://www.sba.unifi.it/upload/policy-oa-2016-1.pdf>)

*Publisher copyright claim:*

Conformità alle politiche dell'editore / Compliance to publisher's policies

Questa versione della pubblicazione è conforme a quanto richiesto dalle politiche dell'editore in materia di copyright.

This version of the publication conforms to the publisher's copyright policies.

La data sopra indicata si riferisce all'ultimo aggiornamento della scheda del Repository FloRe - The above-mentioned date refers to the last update of the record in the Institutional Repository FloRe

(Article begins on next page)

## Modifications on the amino-3,5-dicyanopyridine core to obtain multifaceted adenosine receptor ligands with antineuropathic activity

Marco Betti, Daniela Catarzi, Flavia Varano, Matteo Falsini, Katia Varani, Fabrizio Vincenzi, Silvia Pasquini, Lorenzo Di Cesare Mannelli, Carla Ghelardini, Elena Lucarini, Diego Dal Ben, Andrea Spinaci, Gianluca Bartolucci, Marta Menicatti, and Vittoria Colotta

*J. Med. Chem.*, **Just Accepted Manuscript** • DOI: 10.1021/acs.jmedchem.9b00106 • Publication Date (Web): 15 Jul 2019

Downloaded from pubs.acs.org on July 22, 2019

### Just Accepted

"Just Accepted" manuscripts have been peer-reviewed and accepted for publication. They are posted online prior to technical editing, formatting for publication and author proofing. The American Chemical Society provides "Just Accepted" as a service to the research community to expedite the dissemination of scientific material as soon as possible after acceptance. "Just Accepted" manuscripts appear in full in PDF format accompanied by an HTML abstract. "Just Accepted" manuscripts have been fully peer reviewed, but should not be considered the official version of record. They are citable by the Digital Object Identifier (DOI®). "Just Accepted" is an optional service offered to authors. Therefore, the "Just Accepted" Web site may not include all articles that will be published in the journal. After a manuscript is technically edited and formatted, it will be removed from the "Just Accepted" Web site and published as an ASAP article. Note that technical editing may introduce minor changes to the manuscript text and/or graphics which could affect content, and all legal disclaimers and ethical guidelines that apply to the journal pertain. ACS cannot be held responsible for errors or consequences arising from the use of information contained in these "Just Accepted" manuscripts.

# Modifications on the amino-3,5-dicyanopyridine core to obtain multifaceted adenosine receptor ligands with antineuropathic activity

Marco Betti,<sup>a</sup> Daniela Catarzi,<sup>a\*</sup> Flavia Varano,<sup>a</sup> Matteo Falsini,<sup>a</sup> Katia Varani,<sup>b</sup> Fabrizio Vincenzi,<sup>b</sup> Silvia Pasquini,<sup>b</sup> Lorenzo di Cesare Mannelli,<sup>c</sup> Carla Ghelardini,<sup>c</sup> Elena Lucarini,<sup>c</sup> Diego Dal Ben,<sup>d</sup> Andrea Spinaci,<sup>d</sup> Gianluca Bartolucci,<sup>a</sup> Marta Menicatti,<sup>a</sup> Vittoria Colotta<sup>a</sup>

<sup>a</sup>*Dipartimento di Neuroscienze, Psicologia, Area del Farmaco e Salute del Bambino, Sezione di Farmaceutica e Nutraceutica, Università degli Studi di Firenze, Via Ugo Schiff, 6, 50019 Sesto Fiorentino, Italy.*

<sup>b</sup>*Dipartimento di Scienze Mediche, Sezione di Farmacologia, Università degli Studi di Ferrara, Via Fossato di Mortara 17-19, 44121 Ferrara, Italy*

<sup>c</sup>*Dipartimento di Neuroscienze, Psicologia, Area del Farmaco e Salute del Bambino, Sezione di Farmacologia e Tossicologia, Università degli Studi di Firenze, Viale Pieraccini, 6, 50139 Firenze, Italy.*

<sup>d</sup>*Scuola di Scienze del Farmaco e dei Prodotti della Salute, Università degli Studi di Camerino, Via S. Agostino 1, 62032 Camerino (MC), Italy.*

**Key words:** G protein-coupled receptors, adenosine receptor ligands, aminopyridine-3,5-dicarbonitriles, ligand-adenosine receptor modeling studies, neuropathic pain.

Corresponding author e-mail: [daniela.catarzi@unifi.it](mailto:daniela.catarzi@unifi.it).

**Abstract.**

A new series of amino-3,5-dicyanopyridines (**1-31**) was synthesized and biologically evaluated in order to further investigate the potential of this scaffold to obtain adenosine receptor (AR) ligands. In general, the modifications performed have led to compounds having from high to good human (h) A<sub>1</sub>AR affinity and an inverse agonist profile. While most of the compounds are hA<sub>1</sub>AR selective, some derivatives behave as mixed hA<sub>1</sub>AR inverse agonists/A<sub>2A</sub> and A<sub>2B</sub> AR antagonists. These latter (compound **9-12**) showed to reduce oxaliplatin-induced neuropathic pain by a mechanism involving the alpha7 subtype of nAChRs, similarly to the non-selective AR antagonist caffeine, taken as reference compound. Along with the pharmacological evaluation, chemical stability of the methyl 3-(((6-amino-3,5-dicyano-4-(furan-2-yl)pyridin-2-yl)sulfanyl)methyl)benzoate **10** was assessed in plasma matrices (rat and human), and molecular modeling studies were carried out to better rationalize the available SARs.

## INTRODUCTION

Adenosine is an endogenous autocoid as regulating the function of every tissue and organ in the body.<sup>1</sup> Under physiological conditions, adenosine is present in the extracellular space at low concentrations which dramatically increase in response to stress. Thus, it interacts with specific G protein-coupled adenosine receptors (ARs), four subtypes currently recognized and termed A<sub>1</sub>, A<sub>2A</sub>, A<sub>2B</sub>, and A<sub>3</sub> ARs. Under physiological conditions, concentration of extracellular adenosine (0.3-1000 nM) is high enough to activate both the A<sub>1</sub> and A<sub>2A</sub> ARs. In contrast, the low affinity A<sub>2B</sub> and A<sub>3</sub> subtypes require higher concentrations of extracellular nucleoside. All ARs affect cAMP levels, A<sub>1</sub> and A<sub>3</sub> receptors being coupled to inhibitory G<sub>i</sub>, and A<sub>2A</sub> and A<sub>2B</sub> receptors to stimulatory G<sub>s</sub> proteins, respectively. Furthermore, A<sub>3</sub> and A<sub>2B</sub> receptors are also coupled to G<sub>q</sub> proteins, leading to the activation of phospholipase C (PLC) and an increase in calcium levels.<sup>1,2</sup> Coupling to other intracellular signaling pathways has also been described.<sup>2</sup> The cloning of the four AR subtypes has allowed for significant progress to be made in the understanding of several facets of AR activity at a molecular level. It is well documented that the activation of ARs can produce a large variety of effects in different tissues and organs. The widely diffused adenosine signaling has left long hypothesize that the regulation of ARs' activity had a high therapeutic potential. However, this ubiquity makes the development of selective AR agonists and antagonists difficult to realize without the occurrence of side effects.<sup>3</sup>

The use of AR agonists and antagonists has been shown to protect against neurodegenerative pathologies such as Alzheimer's and Parkinson's diseases, and also neurological insult caused by spinal cord injury and stroke.<sup>4,5</sup> Experimental evidence supports the use of AR antagonists as well as agonists in the control of inflammatory response, sensory and motor deficits, hyperalgesia, antinociception and excitotoxicity related to specific neurodegenerative disorders.<sup>6-11</sup> Results obtained up to now have allowed the seemingly paradoxical use of agonists and antagonists of the same AR subtype to treat similar pathologies to emerge. These contrasting approaches suggest that the state of disease progression, dosage and time of drug application, drug delivery method and many

other factors could be critical for the design of the most effective therapy. In recent years, there have been significant developments that enhance an understanding of the role of adenosine in nociception. It has emerged that all the four AR subtypes are involved in pain regulation but with different roles.<sup>11</sup> Some experimental evidence suggests the role of both A<sub>1</sub> and A<sub>2A</sub> ARs as key targets for the regulation of pain, leaving however the debate about the pharmacological use of agonists and/or antagonists open.<sup>12-17</sup>

Among the four ARs, the A<sub>1</sub> subtype has been traditionally described as a neuroprotective receptor<sup>18</sup> while the excitatory effect of the A<sub>2A</sub>AR in neurodegeneration has been preferentially reported.<sup>4,5</sup> However, some evidence suggested that prolonged A<sub>1</sub>AR activation may lead to neurodegeneration, leading to hypothesize an apparent A<sub>1</sub>/A<sub>2A</sub> ARs cross-talk.<sup>19</sup> In this situation, the A<sub>1</sub> signaling enhances the A<sub>2A</sub>-mediated neurodegeneration. Also the effect on neurotransmitter release is the opposite: activation of the A<sub>1</sub> subtype is associated with inhibition while the A<sub>2A</sub>AR promotes an increased release.<sup>20</sup>

Since the 1990s, much effort has been devoted to evaluating the pharmacological actions of caffeine, the most consumed psychoactive legal drug in the world.<sup>12</sup> Its neuroprotective effects have been generally ascribed to the blockade of both the A<sub>1</sub> and A<sub>2A</sub> ARs though caffeine works as a non-selective antagonists of all the four AR subtypes in human. In rodents, the lack of affinity only for the A<sub>3</sub>AR was demonstrated.<sup>21</sup> Also the blockade of the A<sub>2B</sub> AR was reported to produce antinociception in several model of pain.<sup>11,13</sup> Caffeine's role in controlling pain has been scarcely considered in the past yet it is being studied increasingly.<sup>12,22-25</sup> However, at present the antinociceptive activity of AR antagonists such as caffeine is in contrast with the more documented pain-protective action exerted by AR agonists, in particular compounds targeting the A<sub>1</sub> subtype.<sup>10,11,15,16,18,19</sup>

In our laboratory, much research has been addressed to the study of AR ligands belonging to different chemical classes<sup>26-37</sup> including the recently reported amino-3,5-dicyanopyridine series.<sup>37</sup> These derivatives were designed as hA<sub>2B</sub>AR agonists although special attention was devoted to deepening

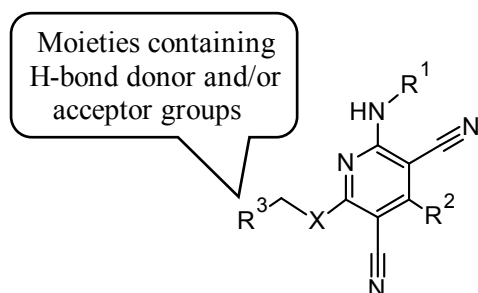
the structure-activity relationships (SARs) of this chemical class. Despite scarce data being reported in the open literature,<sup>38-40</sup> the amino-3,5-dicyanopyridine scaffold has showed to be very versatile for designing AR ligands. In fact, the compounds, whose pharmacological studies are available to the scientific community, may show, in general, not only a wide range of affinities but also different degrees of efficacy at the different ARs. In our recent publication<sup>37</sup> we reported some potent hA<sub>2B</sub> AR receptor partial agonists, belonging to the amino-3,5-dicyanopyridine series, some of which also characterized by good selectivity versus the other AR subtypes. The SAR study highlighted that the 4-(*para*-cyclopropylmethyloxy)phenyl group (Chart 1), with respect to other examined R<sup>2</sup> substituents, emerged as the best one to increase hA<sub>2B</sub> AR activity and selectivity of the amino-3,5-dicyanopyridine compounds. Moreover, moieties bearing H-bond donor and/or acceptor groups at R<sup>3</sup>, able to give polar interactions at this level, proved to be important for A<sub>2B</sub> receptor ligand potency.<sup>41,42</sup> Thus, we decided to further explore this scaffold to evaluate how modifications at the dicyanopyridine core could modulate affinity and selectivity, but also the pharmacological profile of these derivatives at the AR subtypes (Chart 1). Maintaining the characteristics of polarity of the R<sup>3</sup> substituents, that could be important not only for the AR interaction but also activation, different substituents have been evaluated with attention at the R<sup>2</sup> position where less explored heteroaryl moieties were introduced. Further modifications concerned the linker X and the R<sup>1</sup> substituent appended on the amine function.

The new derivatives **1-31** were tested to evaluate their affinities at hA<sub>1</sub>, hA<sub>2A</sub> and hA<sub>3</sub> ARs and their efficacy at the hA<sub>2B</sub>AR. Selected compounds (**1**, **7-11**, **13**, **14**, **17**, **18**, **20**, **23**, **24**, **26**, **28** and **30**) were also analyzed to assess their pharmacological profile at the different ARs. Anticipating our results, it emerges that some amino-3,5-dicyanopyridines reported herein (compounds **9-12**) behave as mixed hA<sub>1</sub> AR inverse agonists/A<sub>2A</sub> and A<sub>2B</sub> AR antagonists. It has to be noted that inverse agonism is slowly establishing its physiological role and also taking a place in drug therapy. In fact, it represents an important expression of drug-receptor interaction different than that of antagonism. An inverse agonist, in addition to blocking the action of the agonist as a neutral antagonist, is able to inhibit the

constitutive activity of the receptor thus showing negative intrinsic activity. However, if the receptor does not display constitutive activity, the inverse agonist behaves as an antagonist. Moreover, new SARs for inverse agonists versus those for antagonists must be sought for and established. Many compounds, endowed with important therapeutic actions and assumed to be G protein-coupled receptor antagonists, have been successively proved to be inverse agonists. Hence, in light of the previously advanced consideration, we glimpsed the possibility that our compounds could act like caffeine and represent promising candidates for the treatment of neuropathic pain. Thus, derivatives **9-12** were pharmacologically evaluated in an *in vivo* mouse model of oxaliplatin-induced neuropathy. Moreover, the stability of the ethyl ester derivatives **10** was assessed in plasma matrices (rat and human). A molecular modeling study of the new amino-3,5-dicyanopyridine derivatives was performed in order to rationalize the obtained pharmacological results.

### Chart 1.

Previously and currently reported amino-3,5-dicyanopyridines as AR ligands.



#### Previously reported

$R^1 = \text{H}, X = \text{S}$   
 $R^2 = 4\text{-R}''\text{-C}_6\text{H}_4$   
 $R = \text{-O-(cyclo)alkyl},$   
 $\text{-O-alkenyl},$   
 $\text{-NHCOCH}_3$

#### Currently reported 1-31

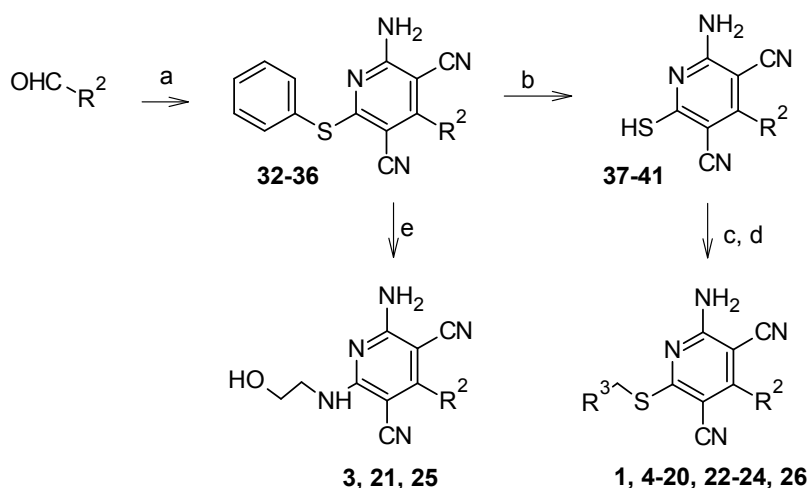
$R^1 = \text{H}, \text{cycloalkyl}, \text{aryl},$   
 $\text{benzyl}, \text{acetyl}$   
 $X = \text{S}, \text{NH}, \text{O}$   
 $R^2 = \text{heteroaryl}$



## RESULTS AND DISCUSSION.

### Chemistry.

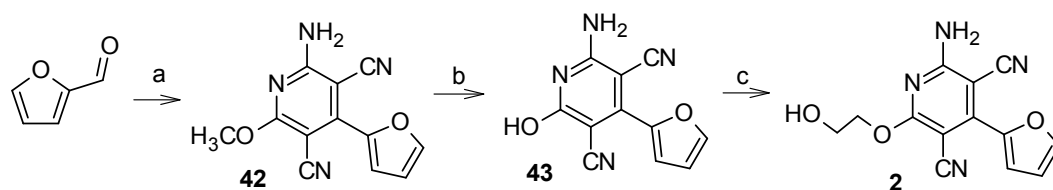
The synthetic routes which provided the amino-3,5-dicyanpyridine derivatives **1-31**<sup>43-45</sup> are depicted in Schemes 1-4. Compounds **1, 3-26** (Scheme 1) were synthesized starting from a one-pot cyclization of the suitable commercially available heteroarylaldehyde with malononitrile and thiophenol in the presence of tetra-n-butylammonium fluoride hydrate (TBAF•H<sub>2</sub>O) to yield the phenylthio-intermediates **32-36**.<sup>46-48</sup> To obtain the free thiols (compounds **37-41**),<sup>49-51</sup> the corresponding 6-phenylthio-derivatives **32-36** were treated with sodium sulfide in anhydrous DMF at 80 °C followed by treatment with 1N HCl. The final compounds **1, 4-20, 22-24, 26** were obtained in high yield by reacting **37-41** with the suitable halides, (all commercially available), in the presence of sodium hydrogen carbonate or potassium hydroxide (compound **5**). Bromomethyl derivatives were used to prepare compounds **1, 2, 9, 10, 18-20, 22-24, 26**, while to yield derivatives **15-17** chloromethyl intermediates were employed, sometimes as hydrochloride. To test the replacement of the thiomethyl bridge with an aminomethyl linker, compounds **3, 21**,<sup>45</sup> **25** were synthesized starting from intermediates **32**,<sup>46</sup> **34**,<sup>46</sup> **36**<sup>48</sup> respectively, taking advantage of the good property of phenylthio group as leaving group in a nucleophilic substitution. The reaction was performed at 100 °C in DMF using 2-aminoethanol as nucleophile.

**Scheme 1.**

R <sup>2</sup>	compd	R <sup>2</sup>	compd
	<b>1,3-17, 32, 37</b>		<b>23, 35, 40</b>
	<b>18, 19, 33, 38</b>		<b>24-26, 36, 41</b>
	<b>20-22, 34, 39</b>		

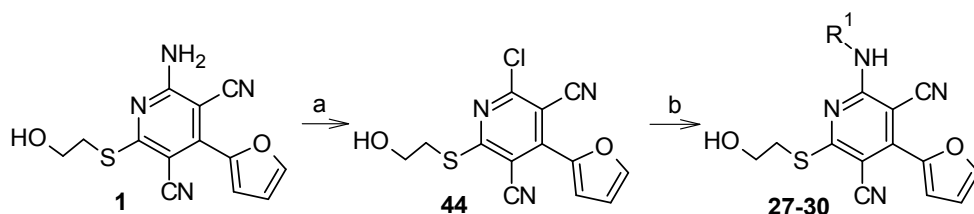
**Reagents and conditions.** a) Malononitrile, thiophenol, TBAF, H<sub>2</sub>O, 80 °C; b) Na<sub>2</sub>S, anhydrous DMF, 80 °C; 1N HCl, rt; c) R<sup>3</sup>CH<sub>2</sub>Br, NaHCO<sub>3</sub>, anhydrous DMF, rt; d) NH<sub>2</sub>COCH<sub>2</sub>Cl, 10% KOH, DMF, rt (compound **5**); e) NH<sub>2</sub>CH<sub>2</sub>CH<sub>2</sub>OH, DMF, 100 °C; (for R<sup>3</sup> substituent details see Table 1).

Pursuing modifications at the methylthio linker, compound **2**, bearing a methoxyethanol chain was synthesized (Scheme 2). One-pot cyclization of commercial 2-furaldehyde with malononitrile in the presence of NaOCH<sub>3</sub> yielded intermediate **42**<sup>52</sup> which was converted into the corresponding hydroxy-analogue **43**<sup>53</sup> by treatment with a mixture of concentrated HCl and glacial acetic acid at 100 °C. Hence, **43** was used as starting material for the coupling reaction with 2-bromoethanol, performed in a microwave reactor, to give the final compound **2**.

**Scheme 2.**

**Reagents and conditions.** a) malononitrile, NaOCH<sub>3</sub>, TBAF, MeOH, reflux; b) 12N HCl, glacial AcOH, 100 °C; c) BrCH<sub>2</sub>CH<sub>2</sub>OH, NaHCO<sub>3</sub>, anhydrous DMF, 80 °C, microwave irradiation.

Replacement of the primary amine function of **1** with suitably substituted amino groups was performed to obtain compounds **27-30** (Scheme 3). Diazotization of the amine derivative **1** using isoamylnitrite as nitrosonium donor compound, followed by Sandmeyer reaction with copper (II) chloride afforded compound **44** in good yields. Thus, the chlorine atom of **44** was easily replaced with commercially available substituted amines yielding the final compounds **27-30**.

**Scheme 3.**

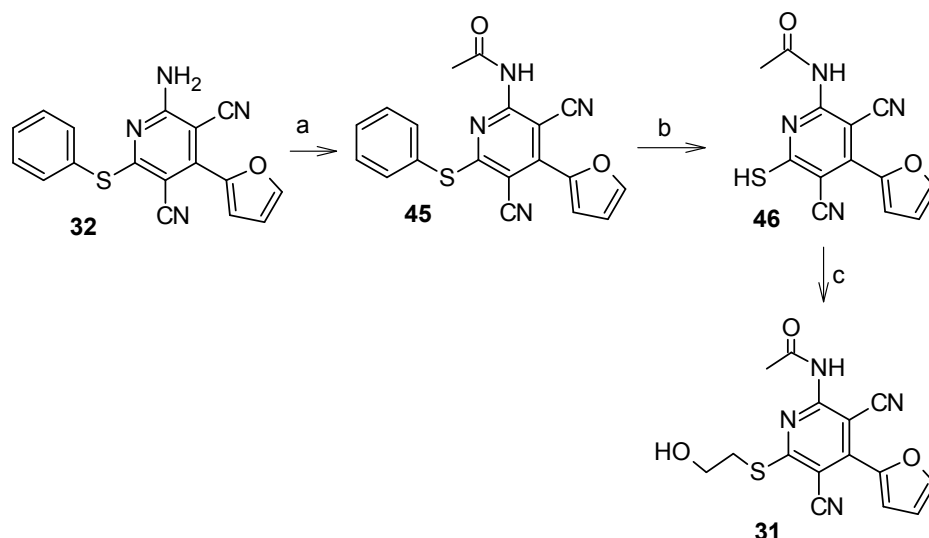
R <sup>1</sup>				
compd	<b>27</b>	<b>28</b>	<b>29</b>	<b>30</b>

**Reagents and conditions.** a) isoamylnitrite, CuCl<sub>2</sub>, CH<sub>3</sub>CN, rt; b) R<sup>1</sup>-NH<sub>2</sub>, anhydrous DMF, rt.

Finally, derivative **31**, bearing an acetyl moiety on the amino group, was synthesized as reported in Scheme 4. Reaction of the phenylthio derivative **32** with acetic anhydride in the presence of pyridine produced **45** which was converted into the corresponding thiol analogue **46**<sup>54</sup> by reacting with sodium

sulfide in anhydrous DMF at 50 °C, followed by treatment with 1N HCl. Then, **46** was used as starting material for the coupling reaction with 2-bromoethanol to afford the target compound **31**.

#### Scheme 4.



**Reagents and conditions.** a) acetic anhydride, pyridine, reflux; b)  $\text{Na}_2\text{S}$ , anhydrous DMF, 50 °C; 1N HCl, rt; c)  $\text{BrCH}_2\text{CH}_2\text{OH}$ ,  $\text{NaHCO}_3$ , anhydrous DMF, rt.

#### Pharmacological Assays

The amino-3,5-dicyanopyridines **1-31** were tested for their affinity at  $\text{hA}_1$ ,  $\text{hA}_{2A}$  and  $\text{hA}_3$  ARs, stably transfected in Chinese Hamster Ovary (CHO) cells, and were also studied as  $\text{hA}_{2B}$  agonists by evaluating their stimulatory effect on cAMP production in CHO cells, stably expressing the  $\text{hA}_{2B}$  AR. Some selected compounds (**1**, **3**, **9-11**, **15**, **18** and **21**) were evaluated also in cAMP production in  $\text{hA}_{2B}$ CHO cells to investigate their antagonistic effect on cAMP production stimulated by 5'-(N-ethyl-carboxamido)adenosine (NECA) 100 nM. Compounds **1**, **3**, **7-24**, **26**, **28**, and **30**, the most interesting in terms of  $\text{hA}_1$ AR affinity, were evaluated for their  $\text{A}_1$  pharmacological profile in the cAMP assay where each compound was tested to assess its capability to modulate Forskolin-stimulated cAMP levels in the absence or presence of the  $\text{A}_1$ AR agonist 2-chloro- $\text{N}^6$ -cyclopentyladenosine (CCPA) (1

nM). Moreover, derivatives **9-11** and **16**, showing good hA<sub>2A</sub>AR affinity, were evaluated for their ability to inhibit the A<sub>2A</sub>AR agonist CGS 21680-stimulated cAMP levels in hA<sub>2A</sub>CHO cells.

All pharmacological data are reported in Tables 1-4 and Figure 1. The selected derivatives **9-12** were also profiled for their effect in an oxaliplatin-induced neuropathic pain model. The results of these experiments are reported in Figures 6-9.

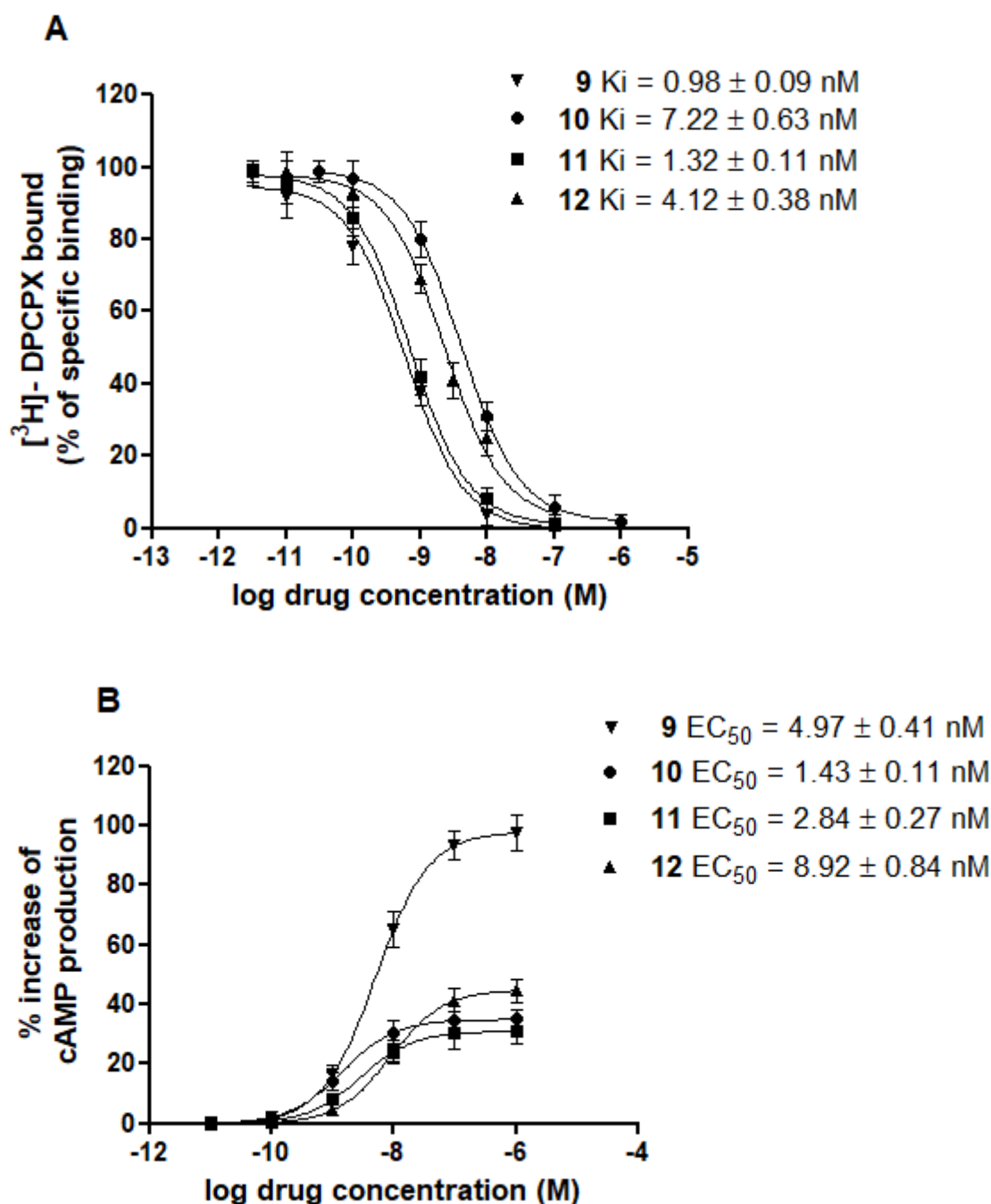
### Structure-activity relationships

The pharmacological data reported in Table 1 show that most of the compounds have, in general, null hA<sub>2B</sub>AR ability in stimulating cAMP production with the only exceptions being derivatives **18**, **20** and **22** that however behave as weak partial agonists. Selected compounds were also evaluated in cAMP assays as hA<sub>2B</sub>AR antagonists (Table 2). In particular, derivatives **9** and **11** are able to inhibit NECA-stimulated cAMP levels with IC<sub>50</sub> values of 152 and 13nM, respectively. In contrast, compounds **1**, **3**, **10**, **15**, **18** and **21** show a percentage of inhibition at the 1 μM concentration in the range 4-40%. Some derivatives (**5**, **6**, **11-13**, **15-17**, **20**, **27** and **31**) interact with the hA<sub>3</sub>AR showing in general K<sub>i</sub> values in the high nanomolar range (Table 1).

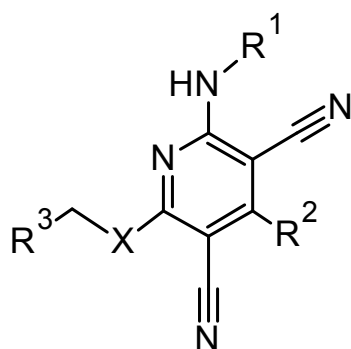
Best results have been obtained in the A<sub>1</sub> and A<sub>2A</sub> AR binding experiments. In particular, all the compounds reported herein, with the only exception being derivatives **3** and **25**, have from high to good hA<sub>1</sub>AR affinity. In particular, some compounds showed K<sub>i</sub> values in the low nanomolar range and in general below 10 nM. Compounds **1**, **7-14**, **16-20**, **22-26**, **28** and **30**, the most interesting in terms of affinity at the hA<sub>1</sub>AR, were evaluated for their pharmacological behavior toward this receptor subtype. The data reported in Table 3 indicated that potencies of the tested compounds correlate well with the K<sub>i</sub> values obtained in the hA<sub>1</sub> binding experiments. All compounds (**1**, **7-14**, **16-20** and **22-26**) were able to increase Forskolin-stimulated cAMP levels in the absence of an agonist, suggesting their inverse agonist profile, with the exception of derivatives **28** (IC<sub>50</sub> = 118 ± 9 nM, E<sub>max</sub> = 100%) and **30** (IC<sub>50</sub> = 76 ± 6 nM, E<sub>max</sub> = 100%) that counteract hA<sub>1</sub>AR agonist CCPA inhibition of Forskolin-stimulated cAMP levels behaving as antagonists. The competition curves of

specific [ $^3\text{H}$ ]-DPCPX binding to  $\text{hA}_1$  AR of compounds **9-12**, selected for in vivo studies, and their effect on forskolin-stimulated c-AMP levels in  $\text{hA}_1\text{AR}$  CHO cells were reported in Figure 1. While some compounds are selective  $\text{hA}_1\text{AR}$  inverse agonists, many derivatives bind also the  $\text{hA}_{2\text{A}}$  receptor, leading to a series of mixed (but not generally balanced)  $\text{hA}_1/\text{A}_{2\text{A}}$  AR ligands. In fact, some compounds bind the  $\text{hA}_1\text{AR}$  better than the  $\text{hA}_{2\text{A}}$  one, thus maintaining a certain selectivity. However, selected compounds (**9-11**, **16**) were also tested in the cAMP functional assay, revealing their antagonistic activity at the  $\text{hA}_{2\text{A}}\text{AR}$  (Table 4). The novel compounds were not able to modulate cAMP levels in wild type CHO cells suggesting the direct involvement of ARs.

Taking into consideration the results that emerged from our previous study on the amino-3,5-dicyanopyridine derivatives<sup>37</sup> together with those reported in the literature on this class of compounds,<sup>38-40</sup> modifications were performed at  $\text{R}^2$  and  $\text{R}^3$  positions (compounds **1-26**). In particular, while poorly investigated heteroaryl substituents were introduced at  $\text{R}^2$ , position  $\text{R}^3$  generally contains groups or atoms able to engage hydrogen bonds with the receptor site, this latter being a condition that seems mandatory for the AR-ligand interaction. First of all, the 2-furanyl substituent was evaluated (compounds **1-17**). In fact, by maintaining the 2-furanyl moiety at  $\text{R}^2$ , different groups were inserted at  $\text{R}^3$  position. In general, the presence of the 2-furanyl moiety at  $\text{R}^2$ , replacing the classical phenyl or phenyl substituted groups usually present at this position, seems to highly influence the interaction or the modality of interaction with the  $\text{hA}_{2\text{B}}\text{AR}$ . In fact, 4-(2-furanyl)-substituted compounds lose the capability to activate this AR subtype, while some, selectively tested derivatives (**9** and **11**) behaved as  $\text{hA}_{2\text{B}}$  antagonists.




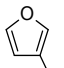
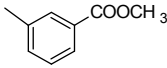
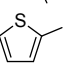
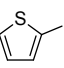
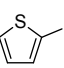
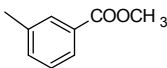
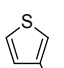
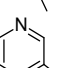
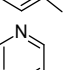
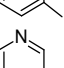
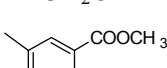
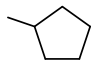
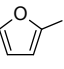

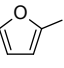
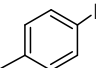
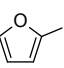
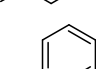
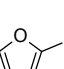
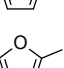
**Figure 1.** Competition curves of specific  $[\text{}^3\text{H}]\text{-DPCPX}$  binding to  $\text{hA}_1\text{ARs}$  of compounds **9-12** (A). Increase of forskolin-stimulated cAMP levels in  $\text{hA}_1\text{AR}$  CHO cells by compounds **9-12** relative to the effect of DPCPX set at 100% (B). Data represent means  $\pm$  SEM of four experiments each performed in triplicate.

**Table 1.** Binding Affinities ( $K_i$ ) at  $hA_1$ ,  $hA_{2A}$  and  $hA_3$  ARs and potencies ( $EC_{50}$ ) at  $hA_{2B}$  ARs.

compd	$R^1$	X	$R^2$	$R^3$	Binding experiments <sup>a</sup>			cAMP assays
					$K_i$ (nM) or I%			$EC_{50}$ (nM) <sup>b</sup>
								Efficacy, <sup>c</sup> %
					$hA_1$ <sup>d</sup>	$hA_{2A}$ <sup>e</sup>	$hA_3$ <sup>f</sup>	$hA_{2B}$
1	H	S		CH <sub>2</sub> OH	57±4	27%	29%	>1000 (7%)
2	H	O		CH <sub>2</sub> OH	632±53	25%	3%	>1000 (11%)
3	H	NH		CH <sub>2</sub> OH	20%	18%	17%	>1000 (1%)
4 <sup>g</sup>	H	S		COOCH <sub>3</sub>	108±9	17%	25%	>1000 (4%)
5 <sup>h</sup>	H	S		CONH <sub>2</sub>	175±12	21%	177±15	>1000 (17%)
6	H	S		CN	93 ± 8	887 ± 84	582 ± 56	>1000 (1%)
7 <sup>g</sup>	H	S		COOCH <sub>2</sub> Ph	86±7	8%	1%	>1000 (10%)
8 <sup>h</sup>	H	S		COPh	23±2	224±21	26%	>1000 (1%)
9	H	S			0.98±0.09	31±3	25%	>1000 (4%)
10	H	S			7.22±0.63	68±3	26%	>1000 (7%)
11	H	S			1.32±0.11	67±6	326±31	>1000 (6%)
12	H	S			4.12±0.38	581±54	611±58	>1000 (1%)
13	H	S			1.02±0.11	93±9	668±64	>1000 (7%)
14	H	S			82±8	1%	11%	>1000 (7%)
15	H	S			40 ± 3	114±10	678 ± 62	>1000 (14%)
16	H	S			1.42±0.15	24±3	948±82	>1000 (1%)
17	H	S			2.71±0.21	108±9	134±12	>1000 (9%)



1  
2  
3  
4  
5  
6  
7  
8  
9  
10  
11  
12  
13  
14  
15  
16  
17  
18  
19  
20  
21  
22  
23  
24  
25  
26  
27  
28  
29  
30  
31  
32  
33  
34  
35  
36  
37  
38  
39  
40  
41  
42  
43  
44  
45  
46  
47  
48  
49  
50  
51  
52  
53  
54  
55  
56  
57  
58  
59  
60

18	H	S		CH <sub>2</sub> OH	19 ± 2	19%	34%	852 ± 81 (32%)
19	H	S			2.11±0.19	96±8	1%	>1000 (7%)
20 <sup>i</sup>	H	S		CH <sub>2</sub> OH	52 ± 5	1%	554 ± 52	885± 79 (69%)
21 <sup>i</sup>	H	NH		CH <sub>2</sub> OH	324 ± 28	33%	29%	>1000 (1%)
22	H	S			2.72±0.21	693 ± 68	15%	982±95 (62%)
23	H	S		CH <sub>2</sub> OH	60 ± 6	9%	33%	>1000 (8%)
24	H	S		CH <sub>2</sub> OH	35 ± 2	7%	22%	>1000 (18%)
25	H	NH		CH <sub>2</sub> OH	1%	1%	8%	>1000 (1%)
26	H	S			1.18±0.11	636±57	8%	>1000 (15%)
27		S		CH <sub>2</sub> OH	742 ± 68	8%	780 ± 72	>1000 (1%)
28		S		CH <sub>2</sub> OH	89±7	30%	30%	>1000 (4%)
29		S		CH <sub>2</sub> OH	10%	1%	8%	>1000 (1%)
30		S		CH <sub>2</sub> OH	65±6	461±42	14%	>1000 (3%)
31	COCH <sub>3</sub>	S		CH <sub>2</sub> OH	243±21	11%	211±18	>1000 (3%)
DPCPX					1.09±0.07	97±8	985±92	>1000 (1%)

<sup>a</sup> K<sub>i</sub> values are means ± SEM of four separate assays, each performed in triplicate. Percentage of inhibition (I%) of specific binding at 1 μM concentration.

<sup>b</sup> EC<sub>50</sub> values are means ± SEM of four separate assays, each performed in triplicate.

<sup>c</sup> Efficacy at 1 μM concentration, in comparison with NECA (1 μM = 100%).

<sup>d</sup> Displacement of specific [<sup>3</sup>H]DPCPX binding at hA<sub>1</sub>ARs expressed in hA<sub>1</sub>CHO cells.

<sup>e</sup> Displacement of specific [<sup>3</sup>H]ZM241385 binding at hA<sub>2A</sub>ARs expressed in hA<sub>2A</sub>CHO cells.

<sup>f</sup> Displacement of specific [<sup>125</sup>I]AB-MECA binding at hA<sub>3</sub>ARs expressed in hA<sub>3</sub>CHO cells.

<sup>g</sup> Reference 43.

<sup>h</sup> Reference 44.

<sup>i</sup> Reference 45.

**Table 2.** Potency at hA<sub>2B</sub> ARs of selected amino-3,5-dicyanopyridine derivatives in the cAMP assay in CHO cells.<sup>a</sup>

compd	IC <sub>50</sub> (nM) <sup>b</sup>
	or I% <sup>c</sup>
<b>1</b>	33%
<b>3</b>	6%
<b>9</b>	152 ± 13
<b>10</b>	25%
<b>11</b>	13 ± 1
<b>12</b>	12%
<b>15</b>	40%
<b>18</b>	38%
<b>21</b>	4%
<b>DPCPX</b>	43 ± 4

<sup>a</sup>cAMP experiments in hA<sub>2B</sub> CHO cells stimulated by 100 nM NECA (EC<sub>50</sub> = 125 ± 15 nM).<sup>b</sup> Potency values (IC<sub>50</sub>) are expressed as means ± SEM of four independent cAMP experiments, each performed in triplicate. <sup>c</sup>Percentage of inhibition (I%) is determined at 1 μM concentration of the tested compound.

1  
2  
3  
4  
5  
6  
7  
8  
9  
10  
11  
12  
13  
14  
15  
16  
17  
18  
19  
20  
21  
22  
23  
24  
25  
26  
27  
28  
29  
30  
31  
32  
33  
34  
35  
36  
37  
38  
39  
40  
41  
42  
43  
44  
45  
46  
47  
48  
49  
50  
51  
52  
53  
54  
55  
56  
57  
58  
59  
60

**Table 3.** Modulation of Forskolin-stimulated cAMP levels of selected amino-3,5-dicyanopyridine derivatives on cyclic cAMP assay in hA<sub>1</sub> CHO cells.<sup>a</sup>

compd	EC <sub>50</sub> (nM) <sup>b</sup>	E <sub>max</sub> (%) <sup>c</sup>	compd	EC <sub>50</sub> (nM) <sup>b</sup>	E <sub>max</sub> (%) <sup>c</sup>
<b>1</b>	128 ± 11	83 ± 6	<b>17</b>	3.41 ± 0.32	30 ± 4
<b>7</b>	192 ± 17	53 ± 5	<b>18</b>	58 ± 5	39 ± 5
<b>8</b>	57 ± 4	29 ± 3	<b>19</b>	4.35 ± 0.38	51 ± 5
<b>9</b>	4.97 ± 0.41	98 ± 7	<b>20</b>	107 ± 9	74 ± 6
<b>10</b>	1.43 ± 0.11	35 ± 4	<b>22</b>	3.85 ± 0.31	56 ± 6
<b>11</b>	2.84 ± 0.27	31 ± 3	<b>23</b>	142 ± 12	62 ± 4
<b>12</b>	8.92 ± 0.84	45 ± 4	<b>24</b>	94 ± 8	75 ± 5
<b>13</b>	4.82 ± 0.39	100 ± 8	<b>26</b>	6.26 ± 0.58	72 ± 6
<b>14</b>	185 ± 16	24 ± 3	<b>DPCPX</b>	1.52 ± 0.12	100 ± 9
<b>16</b>	2.73 ± 0.21	47 ± 5			

<sup>a</sup>Potency values (EC<sub>50</sub>) are expressed as means ± SEM of four independent cAMP experiments, each performed in triplicate. The compounds have been tested on Forskolin at 5 μM concentration.

<sup>b</sup>Potency of the novel compounds to increase Forskolin-stimulated cAMP levels. <sup>c</sup>Efficacy (E<sub>max</sub>) of the novel compounds were normalized by using the E<sub>max</sub> of the reference compound DPCPX (set at 100%) that showed the higher capability to increase cAMP production.

**Table 4.** Potencies at hA<sub>2A</sub>AR of selected amino-3,5-dicyanopyridine derivatives in the cAMP assay in CHO cells.

compd	IC <sub>50</sub> (nM) <sup>a</sup>
<b>9</b>	22 ± 2
<b>10</b>	313 ± 29
<b>11</b>	58 ± 5
<b>16</b>	83 ± 7
<b>DPCPX</b>	132 ± 14

<sup>a</sup>Potency values (IC<sub>50</sub>) of selected compounds to counteract the CGS 21680-stimulated cAMP levels in hA<sub>2A</sub>CHO cells. IC<sub>50</sub> values are expressed as means ± SEM of four independent cAMP experiments, each performed in triplicate.

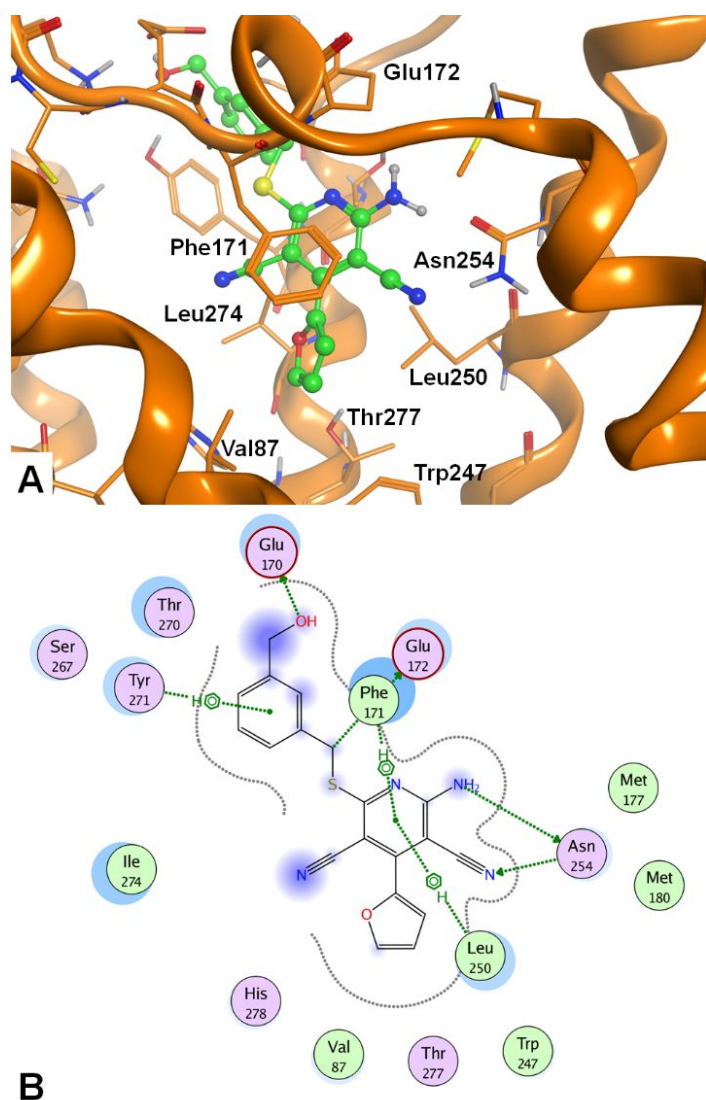
Introduction at R<sup>3</sup> position of small non-aromatic side chains yielded derivatives **1-6** that preferentially bind the hA<sub>1</sub>AR. Hence, the presence of a phenyl moiety on the R<sup>3</sup> substituent (compounds **7, 8**) maintained the hA<sub>1</sub>AR affinity in the nanomolar range, but also the interaction with the hA<sub>2A</sub> receptor was implemented (see compound **8**). Aryl homologation of derivatives **1** and **4-6** produced a high increase of hA<sub>1</sub>AR affinity yielding derivatives **9-11, 13**, all active in the low nanomolar range. Also a substantial improvement of hA<sub>2A</sub> receptor-ligand interaction was observed. This behavior was expected considering that these modifications lead to an increased lipophilicity of the R<sup>3</sup> substituent while its hydrogen bonding properties were maintained. Transformation of the carboxymethyl function of **10** into the corresponding acid **12** maintained the hA<sub>1</sub>AR affinity but reduced the hA<sub>2A</sub> binding. Isosteric replacement of the phenyl moiety at the R<sup>3</sup> position of **10** with a furan ring yielded compound **14** which is endowed with good hA<sub>1</sub>AR affinity and high selectivity versus the other hARs. To evaluate the effect of other heteroaryl moieties at R<sup>3</sup> position, 2-, 3- and 4-pyridinyl groups were introduced yielding compounds **15-17** that showed from high to good hA<sub>1</sub> and hA<sub>2A</sub> AR affinity. The hA<sub>3</sub> receptor binding data of the aminopyridines discussed till now seem to be influenced by the aromatic nature of the R<sup>3</sup> substituent. In fact, compounds **11-13** and **15-17** recovered some affinity for this receptor subtype, the best being compound **17**. Furthermore, modifications at

$R^2$  were performed by replacing the 2-furanyl moiety with a 3-furanyl, 2- and 3-thienyl and 3-pyridinyl group in order to understand how the different heterocyclic substituents could modulate AR binding affinity, selectivity and pharmacological profile of the target compounds. At a glance, these binding data let us to hypothesize that the furan ring at  $R^2$  is important for the anchoring of these aminopyridine derivatives at the  $hA_{2A}$  subtype. In fact, by comparing  $hA_{2A}$   $K_i$  values of the 2- and 3-furanyl derivatives **10** and **19** with the corresponding 4-(2-thienyl) and 4-(3-pyridinyl) compounds **22** and **26**, respectively, it emerged that the  $hA_{2A}$  binding affinity was about ten-fold reduced, while  $K_i$  values at  $hA_1$ AR are highly preserved in the low nanomolar range. As observed for compound **1** and the other 4-(2-furanyl) derivatives bearing a non-aromatic  $R^3$  substituent (**4-6**),  $hA_1$ AR affinity was preserved when other  $R^2$  heteroaryl substituents are present leading also to some selective compounds. Replacing the 6-thiomethyl chain of the derivatives **1**, **20** and **24** with an oxy- (compound **2**) or an amino- (**3**, **21**, **25**) methyl group turned out to be detrimental for  $hA_1$ AR affinity. Finally, the primary 2-amine function of **1** was hindered by insertion of various  $R^1$  substituents to evaluate the role of this position in the binding at all the hARs, especially at the  $hA_1$  one. Cycloalkyl groups (compounds **27**, **28**) or other moieties (**29-31**) that were reported to ameliorate affinity and/or selectivity toward a specific hAR subtype have been taken into consideration.<sup>6</sup> In particular, this information could be important to understand the binding mode of these amino-3,5-dicyanopyridine derivatives at the  $hA_1$  subtype. Not expected was the 13-fold lower  $hA_1$  binding affinity of the 2-(cyclopenthyl)amino derivative **27** with respect to the 2-amino analogue **1**. Moreover, while compounds **28** and **30** bind the  $hA_1$ AR as the lead **1**, the 6-(4-iodophenyl)amino derivative **29** did not show any affinity for any hARs.

In contrast, the presence of a 2-(N-acetylamino) group (compound **31**) enhances the  $hA_3$ AR affinity suggesting that an acyl moiety at this position could be useful for shifting the binding of the amino-3,5-dicyanopyridines toward the  $hA_3$ AR, as extensively demonstrated for other hAR ligands in the literature.<sup>6,27,55</sup>

## Molecular Modeling Studies

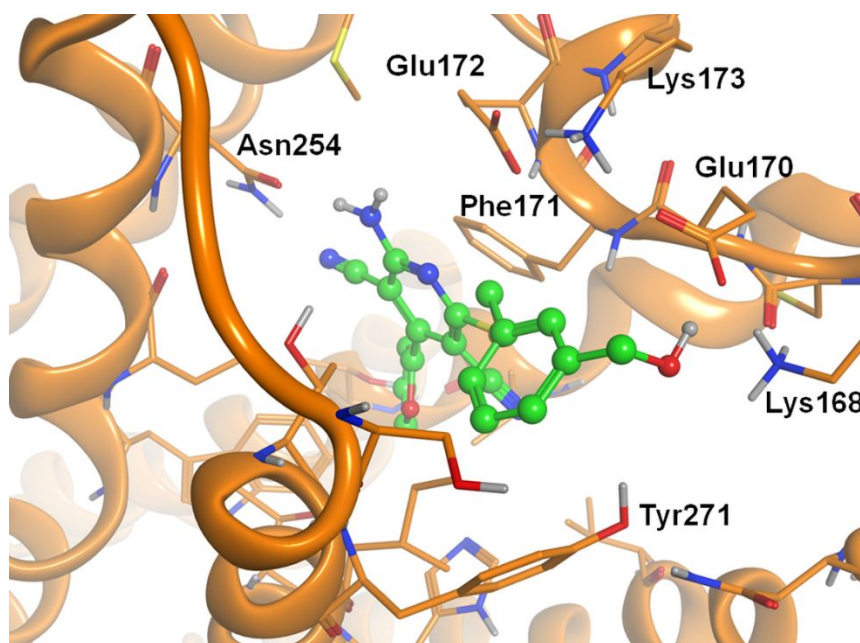
Molecular docking studies were carried out at the hA<sub>1</sub>AR 3D structure to analyze the binding data of the developed compounds. We employed the crystal structure of the hA<sub>1</sub>AR bound to the xanthine-based ligand 4-[3-(8-cyclohexyl-2,6-dioxo-1-propyl-7H-purin-3-yl)propylcarbamoyl]benzenesulfonyl fluoride (DU172) (<http://www.rcsb.org>; pdb code: 5UEN; 3.2-Å resolution<sup>56</sup>). The crystal structure was refined within MOE<sup>57</sup> software and prepared for docking experiments. Docking analyses were performed with CCDC Gold<sup>58</sup> and Autodock software (within PyRx interface).<sup>59-61</sup> Analogous studies for a subset of compounds were performed even at the crystal structure of the hA<sub>2A</sub>AR in complex with the inverse agonist 4-(-2-(7-amino-2-(2-furyl)[1,2,4]triazolo[2,3-a][1,3,5]triazin-5-yl-amino)ethyl)phenol (ZM241385) (pdb code: 4EIY; 1.8-Å resolution<sup>62</sup>) and at a homology model of the hA<sub>3</sub>AR. The binding mode corresponding to the best score generally presents the compounds of interest oriented analogously to the structurally related non-nucleoside agonists docked at other AR subtypes (Figure 2A).<sup>63,64</sup> In detail, the pyridine scaffold gets located in the hA<sub>1</sub>AR cavity in correspondence with the xanthine core of DU172 observed from the hA<sub>1</sub>AR crystal structure, between the side chains of Phe171 (EL2), Leu250<sup>6,51</sup>, and Ile274<sup>7,39</sup>. For clarity, in this section, derivative **9** has been considered as the reference compound to define the position of the substituents on the pyridine nucleus. Thus, starting from the N1 position, the amino and the sulfanyl functions occupy positions 2 and 6, respectively. In general, the exocyclic amino group at the 2-position and the 3-cyano group make a double H-bond interaction with the side chain of Asn254<sup>6,55</sup>, while the 5-cyano group points toward the region between Ala66<sup>2,61</sup>, Ile274<sup>7,39</sup>, and His278<sup>7,43</sup> (Figure 2B).



**Figure 2.** A. Docking conformations of the synthesized compounds at the hA<sub>1</sub>AR (PDB: 5UEN<sup>56</sup>) cavity, taking **9** as template. Key receptor amino acids are indicated. B. Schematic view of the compound-receptor interaction (developed with the Ligand Interaction tool within MOE).

The 6-substituent is oriented toward the entrance of the binding cavity (Figure 3), modulating the interaction with the receptor. Docking results show that the 6-arylalkylthio chain does not remain coplanar with respect to the pyridine ring, as the dihedral angle between the N1 and the C6 atoms, and the S-CH<sub>2</sub> linking group on the 6-substituent results about 60° for most of the compounds. This may be allowed for a thiomethyl- or oxymethyl-containing chain but it gets associated to a much higher

energy when the linker is an amino group due to conjugation effects. Accordingly, binding data show that the hA<sub>1</sub> binding affinity decreases when in the 6-position analogous thiomethyl- or oxymethyl-containing chains are replaced by the corresponding amino-based substituents (i.e. compare compounds **1**, **2** and **3**, respectively). Furthermore, the 6-heteroatom gets located near hydrophobic residues like Ile274<sup>7,39</sup>; this may explain while the sulphur-based chains lead to a higher hA<sub>1</sub> affinity with respect to the corresponding oxygen-based substituents, which are characterized by higher polarity.

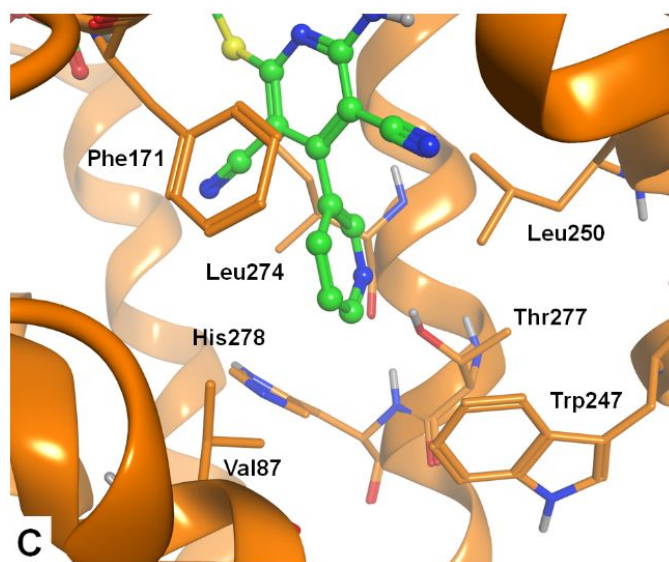
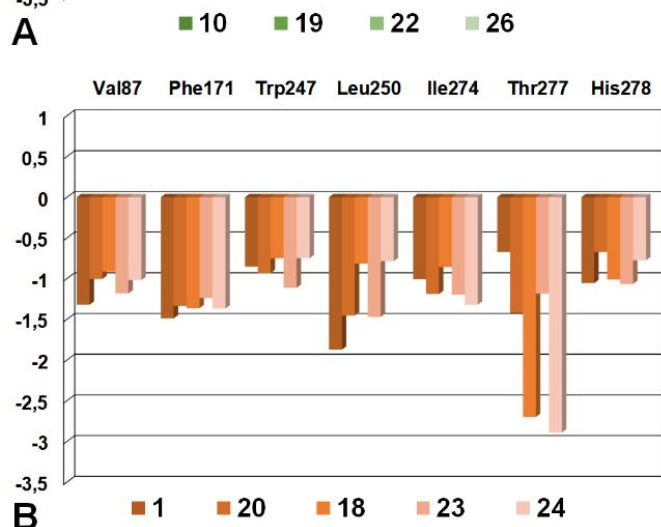
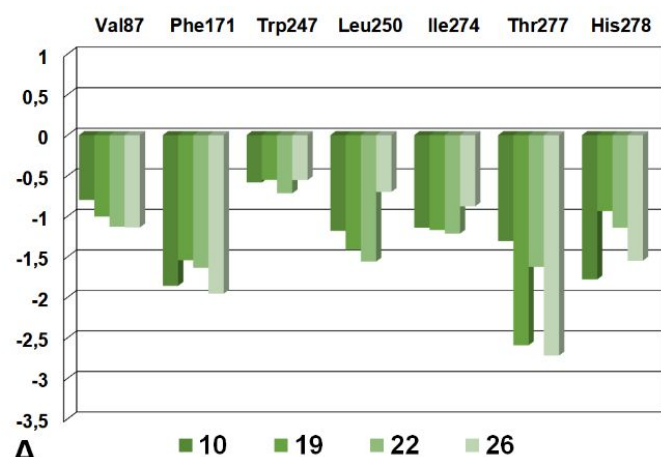


**Figure 3.** Top-view of the docking conformations of the synthesized compounds at the hA<sub>1</sub>AR (PDB: 5UEN<sup>56</sup>) binding site, taking **9** as example: detailed view of the interaction between the 6-substituent and the receptor aminoacids at the entrance of the binding cavity.

In general, compounds bearing a R<sup>3</sup> substituent that contains an aromatic ring functionalized with a polar function (i.e. compounds **9-13** and **15-17**) are endowed with the highest affinity at the hA<sub>1</sub>AR. As shown in Figure 3 for compound **9**, this polar group (the hydroxymethyl in this case) makes interactions with polar residues which are present at the entrance of the binding cavity. In fact, the



presence of polar groups bearing H-bond acceptor or donor functions makes it possible to give interaction with polar amino acids such as Ser267<sup>7,32</sup> or with both positively or negatively charged residues such as Lys168 and Glu170 (both belonging to the EL2 segment), gaining in both cases a good affinity for the hA<sub>1</sub> receptor. In particular, the presence of a polar group at the meta-position of the aromatic R<sup>3</sup> ring allows the polar function to interact with polar residues in the binding pocket, considering various orientations of the aromatic ring. Even when the R<sup>3</sup> substituent is a nitrogen-containing heterocycle such as the pyridyl ring, the highest affinity is obtained with the polar nitrogen atom inserted at the meta-position of the ring itself (compare the hA<sub>1</sub>AR affinity of **15**, **16**, and **17**). The 4-heterocyclic substituent is inserted in the depth of the cavity, close to residues belonging to TM3, EL2, TM6, and TM7 domains (Val87<sup>3,32</sup>, Phe171, Trp247<sup>6,48</sup>, Leu250<sup>6,51</sup>, Ile274<sup>7,39</sup>, Thr277<sup>7,42</sup>, and His278<sup>7,43</sup>). The chemical-physical profile of the ring appears to modulate the affinity for the hA<sub>1</sub>AR. The affinity data reported in Table 1 indicate that a 4-heterocycle bearing a polar atom at the 3-endocyclic position appears to be more beneficial for the hA<sub>1</sub>AR binding affinity with respect to both a 4-heterocycle containing polar atom at the 2-endocyclic position and a non-polar 4-substituent (considering sets of compounds presenting the same 6-substituent). We analysed these data with the *IF-E 6.0* tool, to calculate the per-residue interaction energies (expressed as kcal mol<sup>-1</sup>; see Experimental section for details). This tool was previously used for analogue analyses at hARs obtaining useful interpretation of the compound activity.<sup>29,34,42,63,65</sup> We considered two sets of compounds that differed only in terms of the 4-heterocycle (first set: **10**, **19**, **22**, and **26**; second set: **1**, **18**, **20**, **23**, and **24**). The results are displayed in Figure 4.



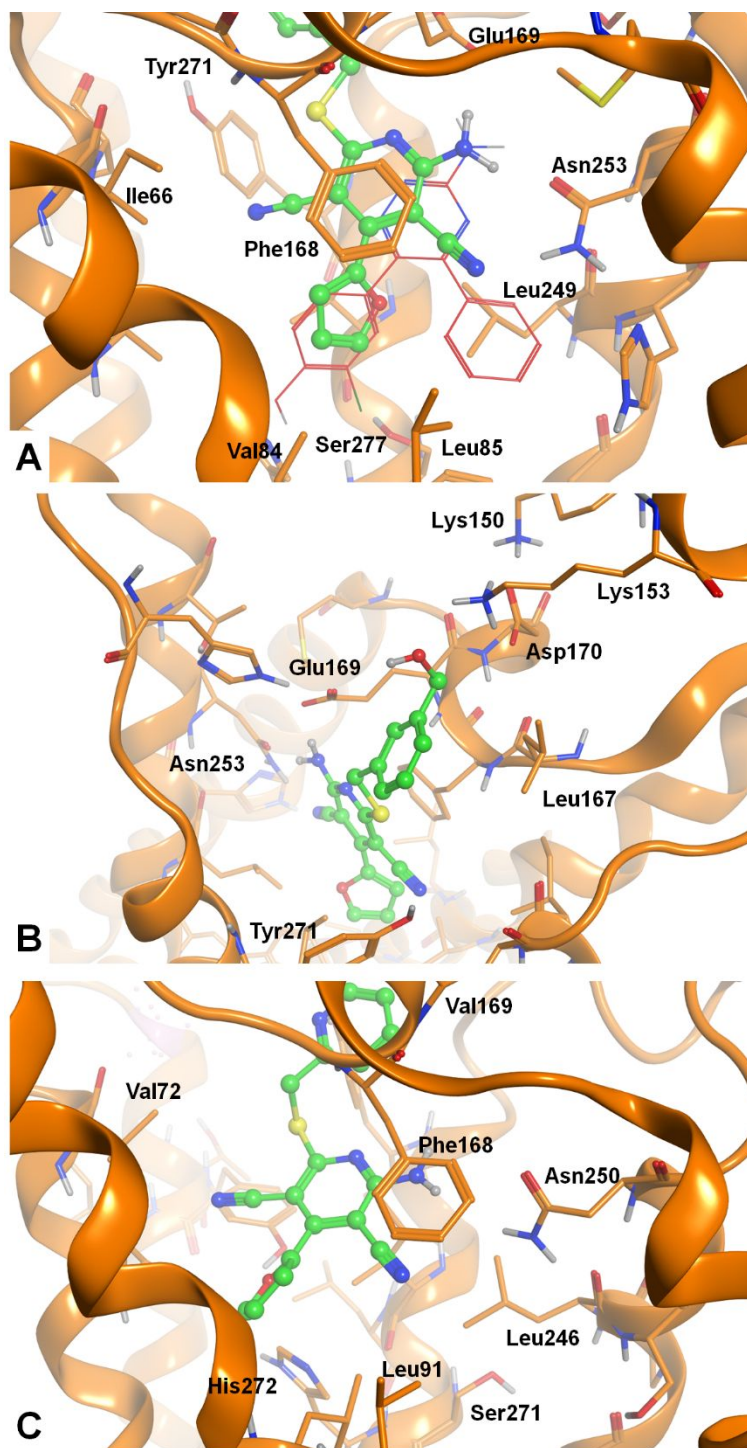
**Figure 4. A-B.** Ligand-target interaction energies calculated with the *IF-E 6.0* tool within MOE (see text for details) for sets of compounds differing only based on the 4-substituent. The receptor's amino acids located close to the 4-substituent were considered and are displayed in panel C. Data are represented as kcal mol<sup>-1</sup>. The results show a significant interaction with Thr277<sup>7,42</sup> for residues

presenting a polar atom at the 3-endocyclic position within the 4-substituent (i.e. **19** and **26** in the first set and **18** and **24** in the second set). C. Detail of the ligand-target interaction at the 4-substituent (compound **26** is shown in this figure). The key residues (PDB: 5UEN<sup>56</sup>) involved in this interaction are displayed and indicated.

It may be observed that the compounds presenting a 4-heterocycle containing a polar atom at the 3-endocyclic position have higher interaction with the Thr277<sup>7,42</sup> residue with respect to the other analogues (i.e. **19** and **26** vs **22** and **10**, or **18**, **24** and **23** vs **1** and **20**). The interaction of the 4-moiety with the residues in its proximity presents analogous trends within each set of compounds. Figure 4 shows the general position of the 4-substituent within the binding cavity and the residues present in its proximity. Among the various residues, the 3-position of the 4-heterocycle moves in proximity to the hydroxyl group of the Thr277<sup>7,42</sup> sidechain.

Docking experiments were performed also at the hA<sub>2A</sub>AR crystal structure and at a hA<sub>3</sub>AR homology model with the same protocol used at the hA<sub>1</sub>AR. Compounds endowed with affinity for these receptor subtypes were considered in this task. Docking results at the hA<sub>2A</sub>AR show an analogue binding mode of the analysed compound **9** at the receptor cavity with respect to the docking conformations at the hA<sub>1</sub>AR (Figure 5 shows an hA<sub>2A</sub>AR-compound **9** complex as example). Analogous considerations made for the 6-substituent at the hA<sub>1</sub>AR may be applied at the hA<sub>2A</sub>AR and this may be due to the presence in the hA<sub>2A</sub>AR of residues having analogous position and chemical-physical profile with respect to the hA<sub>1</sub>AR amino acids interacting with the 6-substituent (i.e. Lys153, Glu169, and Asp170 in hA<sub>2A</sub>AR compared to Lys168, Glu170, and Glu172 in hA<sub>1</sub>AR; Figure 5B). Even the affinity trend is conserved as the most potent compounds at the A<sub>1</sub>AR are endowed with the highest hA<sub>2A</sub>AR affinity, even if the activity at the latter receptor is generally lower. Higher hA<sub>1</sub>AR selectivity is observed based on the kind of heterocycle inserted at the 4-position, where the presence of a thienyl or a pyridyl group leads to a significant decrease of the hA<sub>2A</sub>AR affinity with respect to the furanyl moiety. Figure 5A shows that the position of the 4-heterocycle

corresponds to the one of the 2-chlorophenol substituent of the 3-amino-1,2,4-triazine derivative co-crystallized with the hA<sub>2A</sub>AR (pdb code: 3UZC).<sup>66</sup>



**Figure 5.** A. Docking conformations of the synthesized compounds at the hA<sub>2A</sub>AR cavity, taking compound **9** (green) as template. Key receptor amino acids are indicated. The position of the 4-

heterocycle corresponds to the one of the 2-chlorophenol substituent of the 3-amino-1,2,4-triazine derivative (red) co-crystallized with the hA<sub>2A</sub>AR (pdb code: 3UZC<sup>66</sup>). **B.** Top-view of the docking conformations of the synthesized compounds at the A<sub>1</sub>AR cavity, taking compound **9** as example: detailed view of the interaction between the 6-substituent and the receptor aminoacids at the entrance of the binding cavity. **C.** Binding mode of compound **17** at the hA<sub>3</sub>AR cavity, analogue to the top-score docking conformations at the hA<sub>1</sub>AR and hA<sub>2A</sub>AR. Key receptor residues are indicated. This binding mode was observed only for some of the analyzed derivatives at the hA<sub>3</sub>AR cavity.

Docking results at a hA<sub>3</sub>AR homology model showed different behavior of the analyzed molecules at the binding cavity and a conserved binding mode for these molecules could not be depicted. The above described binding mode was observed only for a few molecules at this receptor cavity (Figure 5C). The top-score docking conformations make the compounds generally located more externally respect to the other hAR cavities. The lack of positively or negatively charged residues in proximity to the 6-substituent (with respect to that observed at the other hARs) could have a role in stabilizing the compounds in a slightly displaced position with respect to the hA<sub>1</sub> and hA<sub>2A</sub> ARs, with a consequent loss of binding interaction for several derivatives that are able to still bind the hA<sub>2A</sub>AR even if with lower affinity than the hA<sub>1</sub>AR.

Docking results at the hA<sub>1</sub>AR presented the 2-amino function of these compounds as being located almost in correspondence to the 6-amine of Ado/NECA compounds co-crystallized with the hA<sub>2A</sub>AR.<sup>67</sup> Given that some reference A<sub>1</sub>AR agonists were obtained by inserting cycloalkyl groups at the *N*<sup>6</sup>-position of Ado (i.e. *N*<sup>6</sup>-cyclopentyladenosine or CPA) and in general the presence of alkyl or cycloalkyl groups led to an improvement of the hA<sub>1</sub>AR affinity, we have modified compound **1** by inserting an alkyl/cycloalkyl/arylalkyl substituent on the 2-amino group. As reported in Table 1, differently from what was expected, this modification did not produce an improvement of the hA<sub>1</sub>AR affinity, leading to a significant decrease in some cases. Docking results of these compounds at the hA<sub>1</sub>AR showed that the presence of a substituted 2-amino group led the compounds to be oriented in

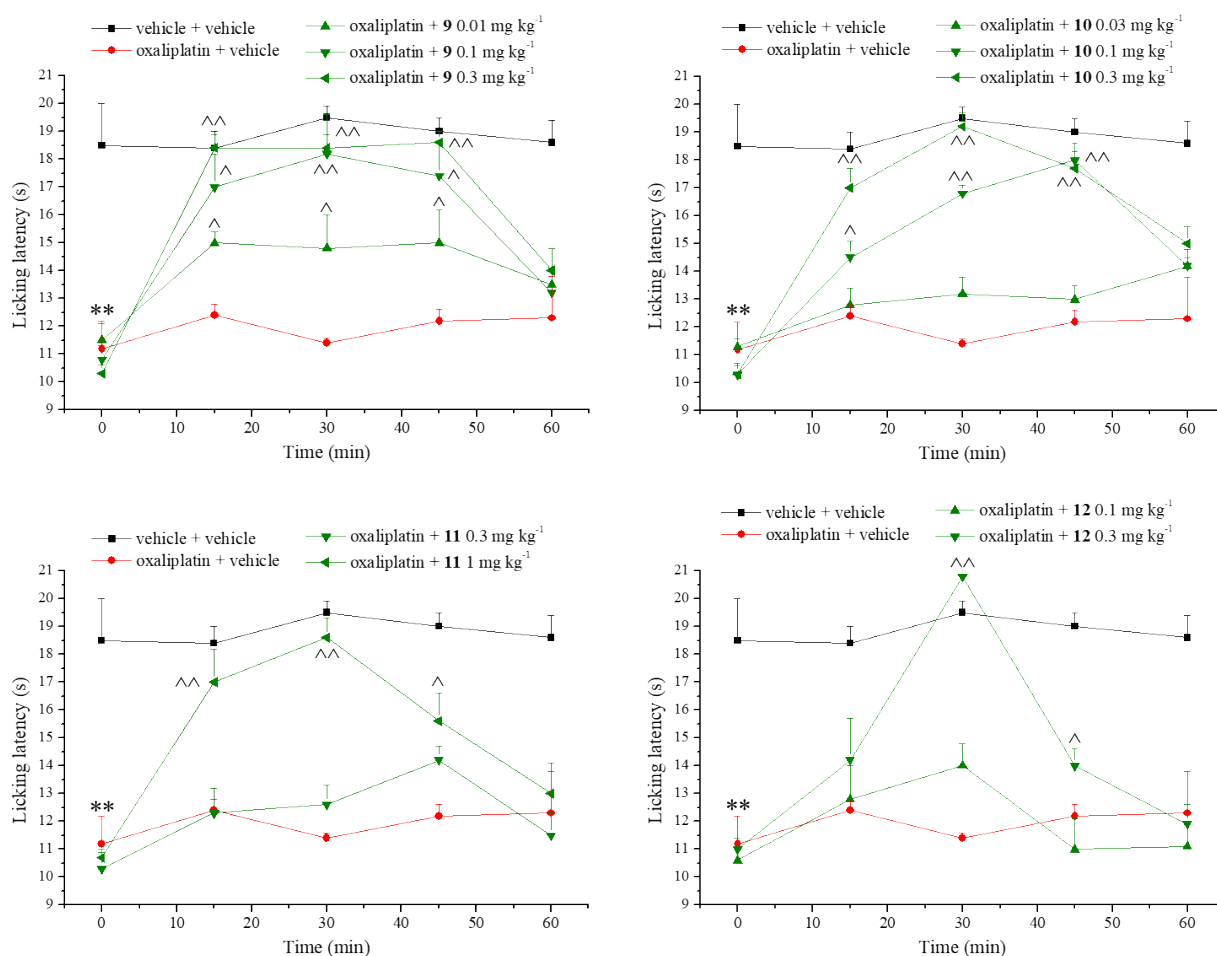
the pocket in several ways, but not in the above-described conformation which is adopted by the 2-unsubstituted molecules (i.e. compound **1** itself). Also, a preferred arrangement for this set of compounds could not be depicted.

### Behavioral studies in the oxaliplatin-induced neuropathy model

It has been reported that non-selective blockade of ARs exerted by caffeine, especially of A<sub>1</sub> and A<sub>2A</sub> subtypes, could be related to its well-known neuroprotective effects.<sup>11,13,21</sup> In light of this hypothesis, four selected compounds, **9-12**, were studied in an *in vivo* mouse model of oxaliplatin-induced neuropathy. In particular, the pain relieving effect induced by a single oral (*per os*, p.o.) administration of different doses of these compounds was evaluated. The pain threshold of mice, evaluated as hypersensitivity to a cold, non-noxious, stimulus (allodynia-like measurements; Cold plate test)<sup>68</sup> was progressively reduced by a daily treatment with oxaliplatin (2.4 mg kg<sup>-1</sup> intraperitoneally - ip). On day 15, licking latency dropped to 10.8 ± 0.8 s when compared to that of control mice (18.5 ± 1.5 s) treated with the vehicle (Figure 6). The acute administration of compound **9** was able to elicit a significant increase of the licking latency, starting from 0.01 mg kg<sup>-1</sup>. The higher doses, 0.1 and 0.3 mg kg<sup>-1</sup>, induced progressively enhanced effects, reaching a complete reversion of hypersensitivity between 15 and 45 min after administration. Similarly, **10** (0.1 and 0.3 mg kg<sup>-1</sup>) evoked full pain relief; the onset was at 15 min, peaking between 30 and 45 min. Compound **11** was effective when 1 mg kg<sup>-1</sup> was administered, whereas the lower dose (0.3) was inactive. In comparison, **12** was more potent than **11**, even if the onset was delayed by 30 min (Figure 6).

All these compounds showed the characteristic profile of inverse agonist of the A<sub>1</sub> receptor and antagonist for the A<sub>2A</sub> subtype. The pharmacodynamic possibility to negatively modulate both the A<sub>1</sub> and A<sub>2A</sub> receptor subtypes suggests analogies with caffeine. Several biological effects of the natural xanthine are mediated by the antagonism to the adenosine receptors.<sup>69</sup> Caffeine-dependent

antinociception can be attributed to the blockade of the  $hA_{2A}$ ,<sup>24</sup> and the  $A_1$ <sup>73</sup> subtypes suggesting the relevance of both these mechanisms in the efficacy of our compounds.



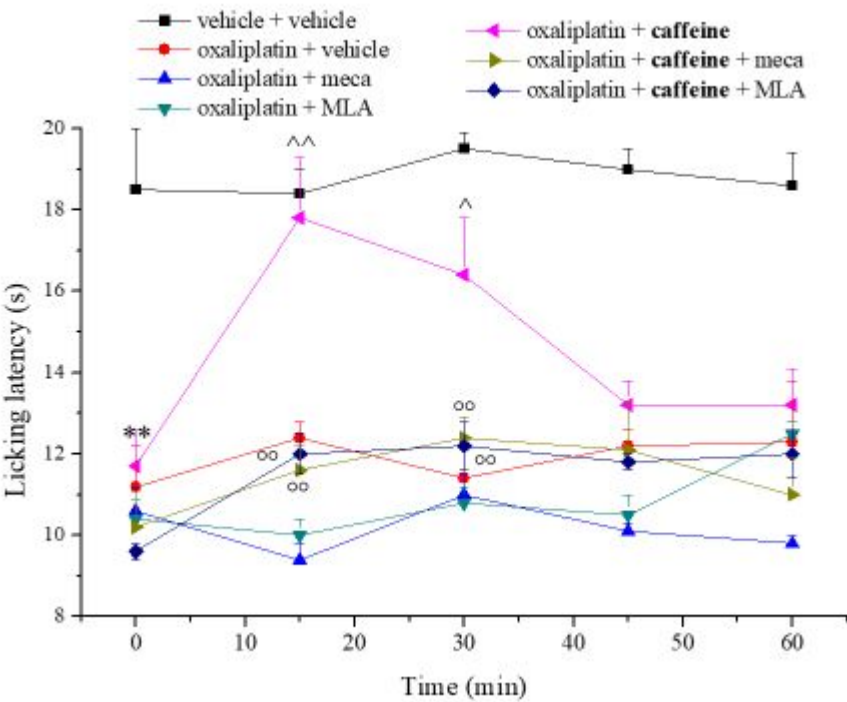
**Figure 6.** Effects of selected compounds against neuropathic pain in mice. Neuropathy was induced by repeated i.p. injection of oxaliplatin (2.4 mg kg<sup>-1</sup>, daily). The hypersensitivity to a cold thermal stimulus was measured on day 15 by the Cold plate test (latency to pain related behaviors as paw lifting or licking). Compounds 9-12 were administered p.o, measurements were performed 15, 30, 45, and 60 min after. Control mice were treated with vehicle. Each value represents the mean of 10 mice per group, performed in 2 different experimental sets. \*\*P < 0.01 vs vehicle + vehicle treated mice. ^P < 0.05 and ^^P < 0.01 vs oxaliplatin + vehicle treated mice.

To validate the hypothesis of similarity, caffeine (10 mg kg<sup>-1</sup> p.o.) was also tested and a significant decrease of oxaliplatin-mediated hypersensitivity was generated (Figure 7). It is worth noting that both A<sub>1</sub> and A<sub>2A</sub> receptors have presynaptic and postsynaptic location; acting at presynaptic heteroreceptors they may modulate neurotransmitter release from dopamine, serotonin<sup>70,71</sup> and acetylcholine (ACh) terminals.<sup>72</sup> In particular, caffeine, via blockade of inhibitory presynaptic adenosine receptors, was able to induce a central cholinergic analgesia by ACh increase.<sup>73</sup> The present results show, for the first time, that the efficacy of caffeine against neuropathic pain is mediated by the cholinergic system. In accordance with previous results that individuated the main relevance of cholinergic signaling in neuropathic condition in the nicotinic component,<sup>74</sup> the caffeine effect was blocked by the non-specific nAChR (nicotinic ACh receptor) antagonist mecamylamine (meca; Figure 7). More specifically, caffeine reduced oxaliplatin-induced pain by a mechanism involving the alpha7 subtype of nAChRs in accordance with previously published data about the role of alpha7 nAChR in chemotherapy-induced neuropathy,<sup>75</sup> since its activity was lost in the presence of the selective alpha7 nAChR antagonist methyllycaconitine (MLA).

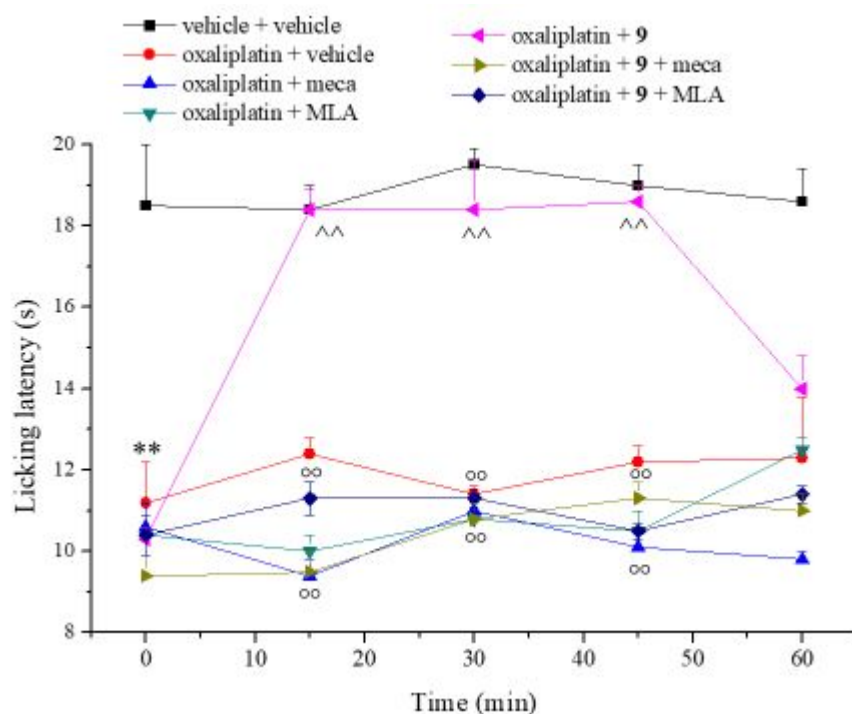
Following this reasoning, we hypothesized a similar mechanism for the new synthesized compounds. The effect of nAChR antagonists were tested on the particularly active compounds **9** and **10**. As shown in Figures 8 and 9, the anti-neuropathic effect of **9** and **10** were completely blocked by both meca and MLA. Involvement of the positive modulation of alpha7 nAChR in the pharmacodynamic mechanism of the new derivatives is proposed.



1  
2  
3  
4  
5  
6  
7  
8  
9  
10  
11  
12  
13  
14  
15  
16  
17  
18  
19  
20  
21  
22  
23  
24  
25  
26  
27  
28  
29  
30  
31  
32  
33  
34  
35  
36  
37  
38  
39  
40  
41  
42  
43  
44  
45  
46  
47  
48  
49  
50  
51  
52  
53  
54  
55  
56  
57  
58  
59  
60

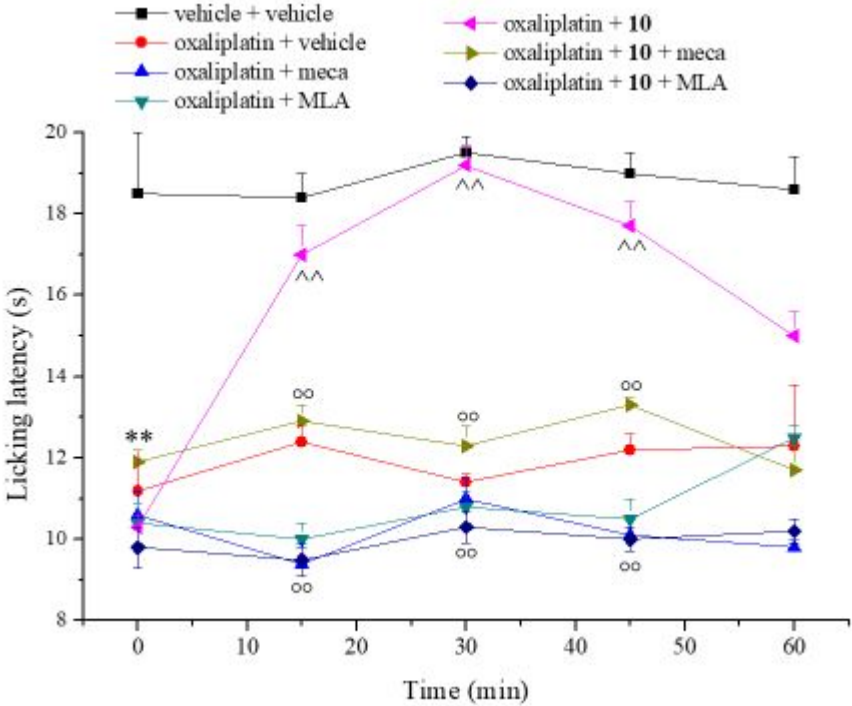


**Figure 7.** Effects of caffeine against neuropathic pain in mice. Role of nAChRs. Neuropathy was induced by repeated i.p. injection of oxaliplatin (2.4 mg kg<sup>-1</sup>, daily). The hypersensitivity to a cold thermal stimulus was measured on day 15 by the Cold plate test (latency to pain related behaviors as paw lifting or licking). Caffeine was administered p.o. at 10 mg kg<sup>-1</sup>. The non-selective nAChR antagonist mecamylamine (meca; 2 mg kg<sup>-1</sup> i.p.) and the selective alpha7 nAChR antagonist methyllycaconitine (MLA; 6 mg kg<sup>-1</sup> i.p.) were administered 15 min before caffeine. Measurements were performed overtime after the injection of caffeine or vehicle (in control mice). Values are reported as mean of 10 mice per group (two different experimental sets). \*\*P < 0.01 vs vehicle + vehicle treated mice. ^P < 0.05 and ^^P < 0.01 vs oxaliplatin + vehicle treated mice. °°P < 0.01 vs oxaliplatin + caffeine treated mice.



**Figure 8.** Effects of nicotinic antagonists on compound **9** anti-hyperalgesic efficacy. Neuropathy was induced by repeated i.p. injection of oxaliplatin ( $2.4 \text{ mg kg}^{-1}$ , daily). The hypersensitivity to a cold thermal stimulus was measured on day 15 by the Cold plate test (latency to pain related behaviors as paw lifting or licking). The non-selective nAChR antagonist mecamylamine (meca;  $2 \text{ mg kg}^{-1}$  i.p.) and the selective  $\alpha 7$  nAChR antagonist methyllycaconitine (MLA;  $6 \text{ mg kg}^{-1}$  i.p.) were administered 15 min before **9** ( $0.3 \text{ mg kg}^{-1}$  p.o.). Measurements were performed overtime after the injection of **9** or vehicle (in control mice). Values are reported as mean of 10 mice per group (two different experimental sets). \*\* $P < 0.01$  vs vehicle + vehicle treated mice. ^ $P < 0.05$  and ^^ $P < 0.01$  vs oxaliplatin + vehicle treated mice. oo $P < 0.01$  vs oxaliplatin + **9** treated mice.

1  
2  
3  
4  
5  
6  
7  
8  
9  
10  
11  
12  
13  
14  
15  
16  
17  
18  
19  
20  
21  
22  
23  
24  
25  
26  
27  
28  
29  
30  
31  
32  
33  
34  
35  
36  
37  
38  
39  
40  
41  
42  
43  
44  
45  
46  
47  
48  
49  
50  
51  
52  
53  
54  
55  
56  
57  
58  
59  
60



**Figure 9.** Effects of nicotinic antagonisms on **10** anti-hyperalgesic efficacy. Neuropathy was induced by repeated i.p. injection of oxaliplatin (2.4 mg kg<sup>-1</sup>, daily). The hypersensitivity to a cold thermal stimulus was measured on day 15 by the Cold plate test (latency to pain related behaviors as paw lifting or licking). The non-selective nAChR antagonist mecamylamine (meca; 2 mg kg<sup>-1</sup> i.p.) and the selective alpha7 nAChR antagonist methyllycaconitine (MLA; 6 mg kg<sup>-1</sup> i.p.) were administered 15 min before **10** (0.3 mg kg<sup>-1</sup> p.o.). Measurements were performed overtime after the injection of **10** or vehicle (in control mice). Values are reported as mean of 10 mice per group (two different experimental sets). \*\*P < 0.01 vs vehicle + vehicle treated mice. ^P < 0.05 and ^^P < 0.01 vs oxaliplatin + vehicle treated mice. °°P < 0.01 vs oxaliplatin + **10** treated mice.

### Chemical stability study

This study was devoted to establishing the chemical stability of the carboxylate ester **10**. In fact, it is well-known that the ester group can be susceptible to hydrolysis by the plasma enzymes. Therefore, to rule out that the observed pharmacological/biological activity was related to the formation of its metabolite, a series of experiments concerning the stability of compound **10** were performed. Due to the analyte concentration levels used in the stability test, the degradation analyses were performed by the LC-MS/MS method operating in the multiple reaction monitoring (MRM) mode. The instrumental conditions are reported in the Experimental Procedures section.

*Degradation profiles.* The stability of compound **10** was evaluated by monitoring the variation of its concentration at different incubation times. By plotting these data (analyte concentrations vs the incubation time), its respective degradation profiles in PBS, in human and in rat plasma matrices were obtained (see Supporting Information). In order to summarize all experimental data, the half-life values of studied compounds were reported in Table 5.

**Table 5.** Half life ( $t_{1/2}$ ) of studied compound in human and rat plasma samples

Compd	Human Plasma	Rat Plasma
	$t_{1/2} \pm SD$ (min.)	$t_{1/2} \pm SD$ (min.)
KEE	$100 \pm 12$	n.d.(*)
Enalapril	n.d.(*)	$22 \pm 8$
<b>10</b>	$\geq 240$	$\geq 240$

(\*) n.d.: not determined.

### Conclusion

The amino-3,5-dicyanopyridines reported in this study proved to be potent hA<sub>1</sub>AR inverse agonists, some of which also endowed with good selectivity versus the other hAR subtypes. However, some derivatives (**9-12**) behave as mixed hA<sub>1</sub>AR inverse agonist/A<sub>2A</sub> and A<sub>2B</sub> AR antagonists, thus

suggesting a similar trend as observed in caffeine, psychoactive compound present in widely consumed beverages, whose neuroprotective effects are well known and ascribed to the non-selective blockade of ARs. Evaluation of compounds **9-12** in mice affected by neuropathic pain confirms that these compounds can act like caffeine, thus representing promising candidates for the treatment of persistent pain. In particular, compounds **9-10**, similarly to caffeine, showed to reduce oxaliplatin-induced neuropathy by a mechanism involving the  $\alpha 7$  subtype of nAChRs. Thus, for the first time it has been highlighted that the efficacy of caffeine against neuropathic pain is mediated by the cholinergic system. Moreover, the chemical degradation profiles of the methyl carboxylate ester **10** confirm the stability of this compound at the conditions operated in the oxaliplatin-induced neuropathy assay as showing high half-life values. Moreover, the similar trend obtained in both rat and human plasma matrices could validate the pharmacological model used. The molecular modeling studies provide an interpretation of the affinity data at the hA<sub>1</sub>AR and suggest a possible development of the aminopyridine series considering the combination of the most suitable R substituent with the optimization of the chemical-physical properties of the 4-heterocycle.

## EXPERIMENTAL PROCEDURES

### Chemistry

The microwave-assisted syntheses were performed using an Initiator EXP Microwave Biotage instrument (frequency of irradiation: 2.45 GHz). Analytical silica gel plates (Merck F254), preparative silica gel plates (Merck F254, 2 mm) and silica gel 60 (Merck, 70-230 mesh) were used for analytical and preparative TLC, and for column chromatography, respectively. All melting points were determined on a Gallenkamp melting point apparatus and are uncorrected. Elemental analyses were performed with a Flash E1112 Thermofinnigan elemental analyzer for C, H, N and the results were within  $\pm 0.4\%$  of the theoretical values. All final compounds revealed purity not less than 95%. The IR spectra were recorded with a Perkin-Elmer Spectrum RX I spectrometer in Nujol mulls and

are expressed in  $\text{cm}^{-1}$ . NMR spectra were recorded on a Bruker Avance 400 spectrometer (400 MHz for  $^1\text{H}$  NMR and 100 MHz for  $^{13}\text{C}$  NMR). The chemical shifts are reported in  $\delta$  (ppm) and are relative to the central peak of the residual non-deuterated solvent, which was  $\text{CDCl}_3$  or  $\text{DMSO-d}_6$ . The following abbreviations are used: s= singlet, d= doublet, t= triplet, q= quartet, m= multiplet, br= broad, ar= aromatic protons., ax=axial, eq=equatorial. Compounds **32**, **34-36**, **37**, **39-41** were synthesized following reported procedures.<sup>46-51</sup>

**Procedure A: Synthesis of the target compounds 1, 4, 6-20, 22-24, 26.** Sodium hydrogen carbonate (2 mmol) and the commercially available halomethyl-derivative (1 mmol) were added to a solution of the suitable mercapto-compound (**37-41**,<sup>49-51</sup> 1 mmol) in anhydrous DMF (1 mL). The reaction mixture was stirred at rt until disappearance of the starting material (TLC monitoring). Then, water was added (25 mL) to precipitate a solid which was collected by filtration and washed with water. The crude product was triturated with  $\text{Et}_2\text{O}$  (5 mL), collected by filtration and purified by crystallization.

**Procedure B: Synthesis of compound 2.** A mixture of compound **43**<sup>53</sup> (0.53 mmol), 2-bromoethanol (0.58 mmol) and sodium hydrogen carbonate (0.79 mmol) in dry DMF (1 mL) was heated at  $80^\circ\text{C}$  under microwave irradiation for 3 h. Then, water (30 mL) was added and the mixture was extracted with  $\text{CH}_2\text{Cl}_2$  (3x25 mL). The collected organic layers were washed with brine (2x20 mL), dried ( $\text{Na}_2\text{SO}_4$ ) and evaporated under reduced pressure to yield a pale green solid that was purified by preparative TLC on silica gel, using  $\text{CH}_2\text{Cl}_2/\text{MeOH}$  9:1 as eluent and then recrystallized.

**Procedure C: Synthesis of 4-substituted-2-amino-6-((2-hydroxyethyl)amino)pyridine-3,5-dicarbonitriles 3, 21, 25.** A solution of the suitable phenylsulfanyl-derivative **32**<sup>46</sup>, **34**<sup>46</sup>, **36**<sup>48</sup> (0.5 mmol) and 2-aminoethanol (2 mmol) in DMF (2 mL) was heated at  $100^\circ\text{C}$  until the disappearance of the starting material (TLC monitoring: silica gel,  $\text{CHCl}_3/\text{MeOH}$  9:1). After cooling at rt, water (10

mL) was added and the resulting precipitate was collected by filtration and washed with water (10 mL) and Et<sub>2</sub>O (5 mL).

**Procedure D: Synthesis of compound 5.**<sup>44</sup> An aqueous solution of KOH (10%, 0.28 mL) was added to a suspension of compound **37**<sup>49</sup> (0.5 mmol) in DMF (2 mL). The reaction mixture was stirred at rt for 5 min and then, chloroacetamide (1 mmol) was added. After stirring at rt for 5h, water (10 mL) was added and the resulting suspension was extracted with EtOAc (3x10 mL). The collected organic layers were dried (Na<sub>2</sub>SO<sub>4</sub>) and the solvent removed under reduced pressure, yielding the crude product which was triturated with Et<sub>2</sub>O (2 mL) and collected by filtration.

**Procedure E: Synthesis of 2-amino-substituted 4-(furan-2-yl)-6-((2-hydroxyethyl)sulfanyl)pyridine-3,5-dicarbonitriles 27-30.** An excess of the suitable primary amine (2.0 mmol) was added to a solution of **44** (1.0 mmol) in anhydrous DMF (0.5 mL) and the mixture was stirred at rt until disappearance of the starting material (TLC monitoring, SiO<sub>2</sub>, EtOAc/CHX/MeOH 6:3:1). Then, water (40 mL) was added affording a solid which was collected by filtration and washed with Et<sub>2</sub>O (5 mL).

**2-Amino-4-(furan-2-yl)-6-((2-hydroxyethyl)sulfanyl)pyridine-3,5-dicarbonitrile (1).** Prepared from **37** according to Procedure A. TLC: SiO<sub>2</sub>, EtOAc/CHX/MeOH 6:3:1; yield 63%; mp 171-173 °C (EtOAc/CHX). <sup>1</sup>H NMR (DMSO-d<sub>6</sub>) 8.12-8.11 (m, 1H, Ar), 7.99 (br s, 2H, NH<sub>2</sub>), 7.39 (d, *J*=3.6 Hz, 1H, Ar), 6.83 (dd, *J*=1.72, 3.6 Hz, 1H, Ar), 4.99 (t, *J*=5.4 Hz, 1H, OH), 3.65 (q, *J*=12 Hz, 2H, CH<sub>2</sub>), 3.33 (t, *J*=6.3 Hz, 2H, CH<sub>2</sub>); IR 3320, 3219, 2212. Anal. Calc. for C<sub>13</sub>H<sub>10</sub>N<sub>4</sub>O<sub>2</sub>S.

**2-Amino-4-(furan-2-yl)-6-(2-hydroxyethoxy)pyridine-3,5-dicarbonitrile (2).** Prepared from **43** according to Procedure B. Yield 56%; mp 207-209 °C (EtOH). <sup>1</sup>H NMR (DMSO-d<sub>6</sub>) 8.09 (s, 1H, Ar), 8.03 (br s, 2H, NH<sub>2</sub>), 7.38 (d, *J*=3.5 Hz, 1H, Ar), 6.84-6.83 (m, 1H, Ar), 4.91 (t, *J*=5.3 Hz, 1H, OH), 4.54-4.17 (m, 2H, OCH<sub>2</sub>), 3.73 (dd, *J*=10.0, 5.2 Hz, 2H, CH<sub>2</sub>). <sup>13</sup>C NMR (DMSO-d<sub>6</sub>) 166.70,

162.20, 146.50, 145.86, 116.47, 116.36, 115.79, 113.19, 79.48, 69.52, 64.57, 59.40 Anal. Calc. for  $C_{13}H_{10}N_4O_3$ .

**2-Amino-4-(furan-2-yl)-6-((2-hydroxyethyl)amino)pyridine-3,5-dicarbonitrile (3).** Prepared from **32** according to Procedure C. Yield 92%; mp: 230-232 °C (EtOH).  $^1H$  NMR (DMSO- $d_6$ ) 8.03 (d,  $J=0.96$  Hz, 1H, Ar), 7.33 (br s, 2H,  $NH_2$ ), 7.24 (d,  $J=0.56$  Hz, 1H, Ar), 7.19 (t,  $J=5.4$  Hz, 1H, NH), 6.78 (dd,  $J=3.5, 1.7$  Hz, 1H, Ar), 4.76 (t,  $J=5.0$  Hz, 1H, OH), 3.54 (q,  $J=11$  Hz, 2H,  $CH_2$ ), 3.47 (q,  $J=11$  Hz, 2H,  $OCH_2$ ). IR 3334, 2204. Anal. Calc. for  $C_{13}H_{11}N_5O_2$ .

**Methyl ((6-amino-3,5-dicyano-4-(furan-2-yl)pyridin-2-yl)sulfanyl)acetate (4).**<sup>43</sup> Prepared from **37** according to Procedure A. TLC:  $SiO_2$ , EtOAc/CHX 1:1; yield 76%; mp 227-229 °C (EtOAc/CHX).  $^1HNMR$  (DMSO- $d_6$ ) 8.12 (d,  $J=1.12$  Hz, 1H, Ar), 8.02 (br s, 2H,  $NH_2$ ), 7.42 (d,  $J=3.5$  Hz, 1H, Ar), 6.84-6.85 (m, 1H, Ar), 4.19 (s, 2H,  $CH_2$ ), 3.68 (s, 3H,  $CH_3$ ). IR 3327, 3218, 2208. Anal. Calc. for  $C_{14}H_{10}N_4O_3S$ .

**2-[[6-Amino-3,5-dicyano-4-(furan-2-yl)pyridin-2-yl]sulfanyl]acetamide (5).** Prepared from **37** according to Procedure D. Yield 73%; mp 271-273 °C dec. (EtOH/DMF).  $^1HNMR$  (DMSO- $d_6$ ) 8.11-8.10 (m, 1H, Ar), 8.00 (br s, 2H,  $NH_2$ ), 7.50 (br s, 1H, NH), 7.41 (d,  $J=3.1$  Hz, 1H, Ar), 7.24 (br s, 1H, NH), 3.87 (s, 2H,  $CH_2$ ), 6.84-6.83 (m, 1H, Ar). IR 3325, 3221, 2208. Anal. Calc. for  $C_{13}H_9N_5O_2S$ .

**2-Amino-6-((cyanomethyl)sulfanyl)-4-(furan-2-yl)pyridine-3,5-dicarbonitrile (6).** Prepared from **37** according to Procedure A. TLC:  $SiO_2$ , EtOAc/CHX/MeOH 7:2:1; yield 43%; mp 297-299 °C (2-methoxyethanol).  $^1H$  NMR (DMSO- $d_6$ ) 8.16 (br s, 2H,  $NH_2$ ), 8.17-8.11 (m, 1H, Ar), 7.51-7.39 (m, 1H, Ar), 6.86 (dd,  $J=3.7, 1.8$  Hz, 1H, Ar), 4.33 (s, 2H,  $CH_2$ ). IR 3404, 3319, 3228, 3313, 2257, 2208. Anal. Calc. for  $C_{13}H_7N_5OS$ .

**Benzyl 2-((6-amino-3,5-dicyano-4-(furan-2-yl)pyridin-2-yl)sulfanyl)acetate (7).** Prepared from **37** according to Procedure A. TLC:  $SiO_2$ , EtOAc/CHX 1:1; yield 30%; mp 222-224 °C (EtOAc/EtOH).  $^1H$  NMR (DMSO- $d_6$ ) 8.12 (s, 1H, Ar), 7.99 (s, 2H,  $NH_2$ ), 7.42 (d,  $J=3.6$  Hz, 1H, Ar), 7.41-7.20 (m, 5H, Ar), 6.85 (dd,  $J=3.6, 1.7$  Hz, 1H, Ar), 5.19 (s, 2H,  $CH_2$ ), 4.28 (s, 2H,  $SCH_2$ );  $^{13}C$



NMR (DMSO- $d_6$ ) 168.41, 166.98, 160.51, 145.44, 144.25, 136.24, 128.85, 128.54, 128.31, 116.99, 116.08, 116.01, 113.35, 89.77, 82.38, 67.10, 32.44. IR 3441, 3314, 3209, 2214, 1732. Anal. Calc. for  $C_{20}H_{14}N_4O_3S$ .

**2-Amino-4-(furan-2-yl)-6-((2-oxo-2-phenylethyl)sulfanyl)pyridine-3,5-dicarbonitrile (8).**<sup>44</sup>

Prepared from **37** according to Procedure A. TLC:  $SiO_2$ , EtOAc/CHX 1:1; yield 47%; mp 251-253 °C (EtOAc).  $^1H$  NMR (DMSO- $d_6$ ) 8.28 (d,  $J=5.7$  Hz, 1H, Ar), 8.08 (t,  $J=6.3$  Hz, 2H, Ar), 7.94 (br s, 2H,  $NH_2$ ), 7.93 (d,  $J=5.5$  Hz, 1H, Ar), 7.71 (dd,  $J=13.4, 6.6$  Hz, 1H, Ar), 7.65-7.52 (m, 2H, Ar), 6.91 (d,  $J=4.8$  Hz, 1H, Ar), 5.01 (d,  $J=5.8$  Hz, 2H,  $CH_2$ ). IR 3485, 3350, 2206, 1618. Anal. Calc. for  $C_{19}H_{12}N_4O_2S$ .

**2-Amino-4-(furan-2-yl)-6-((3-(hydroxymethyl)benzyl)sulfanyl)pyridine-3,5-dicarbonitrile (9).**

Prepared from **37** according to Procedure A. TLC:  $SiO_2$ , EtOAc/CHX 1:1; yield 43%; mp 193-195 °C (EtOAc).  $^1H$  NMR (DMSO- $d_6$ ) 8.24 (s, 1H, Ar), 8.10 (br s, 2H,  $NH_2$ ), 7.90 (t,  $J=1.6$  Hz, 1H, Ar), 7.42 (s, 1H, Ar), 7.37 (d,  $J=7.5$  Hz, 1H, Ar), 7.27 (t,  $J=7.5$  Hz, 1H, Ar), 7.21 (d,  $J=7.5$  Hz, 1H, Ar), 6.87 (s, 1H, Ar), 5.19 (t,  $J=5.7$  Hz, 1H, OH), 4.55-4.43 (m, 4H,  $2CH_2$ ). IR 3398, 3314, 3215, 2214. Anal. Calc. for  $C_{19}H_{14}N_4O_2S$ .

**Methyl 3-(((6-amino-3,5-dicyano-4-(furan-2-yl)pyridin-2-yl)sulfanyl)methyl)benzoate (10).**

Prepared from **37** according to Procedure A. TLC:  $SiO_2$ , EtOAc/CHX/MeOH 7:2:1; yield 62%; mp 208-210 °C (MeOH/2-methoxyethanol).  $^1H$  NMR (DMSO- $d_6$ ) 8.09-8.08 (m, 1H, Ar), 8.00 (br s, 2H,  $NH_2$ ), 7.83-7.85 (m, 3H, Ar), 7.47 (t,  $J=7.72$  Hz, 1H, Ar), 7.38 (d,  $J=3.64$  Hz, 1H, Ar), 6.83 (dd,  $J=1.72, 3.64$  Hz, 1H, Ar), 4.58 (s, 2H,  $CH_2$ ), 3.86 (s, 3H,  $CH_3$ ); IR 2214, 1728. Anal. Calc. for  $C_{20}H_{14}N_4O_3S$ .

**3-(((6-Amino-3,5-dicyano-4-(furan-2-yl)pyridin-2-yl)sulfanyl)methyl)benzamide (11).** Prepared

from **37** according to Procedure A. TLC:  $SiO_2$ , EtOAc/CHX/MeOH 7:2:1; yield 43%; mp: 249-251 °C (EtOH).  $^1H$  NMR (DMSO- $d_6$ ) 8.10 (d,  $J=1.1$  Hz, 1H, Ar), 8.07 (br s, 2H,  $NH_2$ ), 7.98 (s, 1H, Ar), 7.96 (br s, 1H, NH), 7.76 (d,  $J=7.8$  Hz, 1H, Ar), 7.68 (d,  $J=7.7$  Hz, 1H, Ar), 7.49-7.29 (m, 3H, 2Ar +

NH), 6.83 (dd, J=3.6, 1.8 Hz, 1H, Ar), 4.53 (s, 2H, CH<sub>2</sub>). IR 3424, 3360, 3331, 3213, 2210, 1643.

Anal. Calc. for C<sub>19</sub>H<sub>13</sub>N<sub>5</sub>O<sub>2</sub>S.

**3-(((6-Amino-3,5-dicyano-4-(furan-2-yl)pyridin-2-yl)sulfanyl)methyl)benzoic acid (12).**

Prepared from **37** according to Procedure A. TLC: SiO<sub>2</sub>, EtOAc/CHX/MeOH 7:2:1; yield 35%; mp 255-257 °C (EtOH). <sup>1</sup>H NMR (DMSO-d<sub>6</sub>) 13.01 (s, 1H, COOH), 8.10 (d, J=1.0 Hz, 1H, Ar), 8.05 (s, 1H, Ar), 8.13 (br s, 2H, NH<sub>2</sub>), 7.86-7.76 (m, 2H, Ar), 7.44 (t, J=7.7 Hz, 1H, Ar), 7.39 (d, J=3.6 Hz, 1H, Ar), 6.83 (dd, J=3.6, 1.7 Hz, 1H, Ar), 4.58 (s, 2H, CH<sub>2</sub>). IR 3329, 3327, 2214, 1541. Anal. Calc. for C<sub>19</sub>H<sub>12</sub>N<sub>4</sub>O<sub>3</sub>S.

**2-Amino-6-((3-cyanobenzyl)sulfanyl)-4-(furan-2-yl)pyridine-3,5-dicarbonitrile (13).** Prepared from **37** according to Procedure A. TLC: SiO<sub>2</sub>, EtOAc/CHX 1:1; yield 68%; mp 193-195 °C (EtOH). <sup>1</sup>H NMR (DMSO) 8.23 (s, 1H, Ar), 8.15 (br s, 2H, NH<sub>2</sub>), 8.08 (s, 1H, Ar), 7.90 (dd, J=3.6, 1.8 Hz, 1H, Ar), 7.88 (d, J=8.0 Hz, 1H, Ar), 7.72 (d, J=7.7 Hz, 1H, Ar), 7.53 (t, J=7.8 Hz, 1H, Ar), 6.86 (s, 1H, Ar), 4.50 (s, 2H, CH<sub>2</sub>). IR 3410, 3321, 3228, 2227, 2212. Anal. Calc. for C<sub>19</sub>H<sub>11</sub>N<sub>5</sub>OS.

**Methyl 5-(((6-amino-3,5-dicyano-4-(furan-2-yl)pyridin-2-yl)sulfanyl)methyl)furan-2-carboxylate (14).** Prepared from **37** according to Procedure A. TLC: SiO<sub>2</sub>, EtOAc/CHX/MeOH 7:2:1; yield 64%; mp 260-262 °C (acetone). <sup>1</sup>H NMR (DMSO-d<sub>6</sub>) 8.25 (s, 1H, Ar), 8.20 (br s, 2H, NH<sub>2</sub>), 7.91 (s, 1H, Ar), 7.25 (d, J=3.5 Hz, 1H, Ar), 6.88 (s, 1H, Ar), 6.79 (d, J=3.4 Hz, 1H, Ar), 4.62 (s, 2H, CH<sub>2</sub>), 3.80 (s, 3H, CH<sub>3</sub>). IR 3402, 3334, 3240, 2222, 2210. Anal. Calc. for C<sub>18</sub>H<sub>12</sub>N<sub>4</sub>O<sub>4</sub>S.

**2-Amino-4-(furan-2-yl)-6-((pyridin-4-ylmethyl)sulfanyl)pyridine-3,5-dicarbonitrile (15).**

Prepared from **37** according to Procedure A. TLC: SiO<sub>2</sub>, EtOAc/CHX/MeOH 7:2:1; yield 80%; mp 261-262 °C dec. (EtOH/2-metossietanolo). <sup>1</sup>H NMR (DMSO-d<sub>6</sub>) 8.50 (d, J=5.9 Hz, 2H, Ar), 8.10 (d, J=1.5 Hz, 1H, Ar), 8.00 (br s, 2H, NH<sub>2</sub>), 7.54 (d, J=5.9 Hz, 2H, Ar), 7.38 (d, J=3.6 Hz, 1H, Ar), 6.83 (dd, J=1.6 Hz, 3.6 Hz, 1H, Ar), 4.47 (s, 2H, CH<sub>2</sub>). IR 3311, 3171, 2204, 3373, 3314, 3152, 2210, 1728. Anal. Calc. for C<sub>17</sub>H<sub>11</sub>N<sub>5</sub>OS

**2-Amino-4-(furan-2-yl)-6-((pyridin-3-ylmethyl)sulfanyl)pyridine-3,5-dicarbonitrile (16).**

Prepared from **37** according to Procedure A. TLC: SiO<sub>2</sub>, EtOAc/CHX/MeOH 7:2:1; yield 80%; mp

228-230 °C (MeOH). <sup>1</sup>H NMR (DMSO-d<sub>6</sub>) 8.77 (d, J= 2.1 Hz, 1H, Ar), 8.45 (dd, J=4.8, 1.5 Hz, 1H, Ar), 8.89-7.52 (br s, 2H, NH<sub>2</sub>), 8.10 (d, J=1.7 Hz, 1H, Ar), 7.94 (d, J=7.9 Hz, 1H, Ar), 7.38 (d, J=3.6 Hz, 1H, Ar), 7.34 (dd, J=7.8, 4.8 Hz, 1H, Ar), 6.83 (dd, J=3.6, 1.7 Hz, 1H, Ar), 4.49 (s, 2H, CH<sub>2</sub>); IR 3385, 3086, 2206. Anal. Calc. for C<sub>17</sub>H<sub>11</sub>N<sub>5</sub>OS

**2-Amino-4-(furan-2-yl)-6-((pyridin-2-ylmethyl)sulfanyl)pyridine-3,5-dicarbonitrile (17).**

Prepared from **37** according to Procedure A. TLC: SiO<sub>2</sub>, EtOAc/CHX/MeOH 7:2:1; yield 44%; mp 212-214 °C (MeOH). <sup>1</sup>H NMR (DMSO-d<sub>6</sub>) 8.48 (d, J=4.7 Hz, 1H, Ar), 8.11 (br s, 2H, NH<sub>2</sub>), 8.00 (d, J=1.5 Hz, 1H, Ar), 7.76-7.74 (m, 1H, Ar), 7.60 (d, J=7.8 Hz, 1H, Ar), 7.37 (d, J=3.6 Hz, 1H, Ar), 7.34-7.24 (m, 1H, Ar), 6.80 (dd, J=3.6, 1.7 Hz, 1H, Ar), 4.56 (s, 2H, CH<sub>2</sub>); <sup>13</sup>C NMR (DMSO-d<sub>6</sub>) 167.73, 160.59, 150.03, 145.54, 144.30, 137.29, 124.18, 123.00, 116.85, 116.14, 113.29, 89.68, 82.11, 35.95. IR 3389, 3311, 3148, 2206. Anal. Calc. for C<sub>17</sub>H<sub>11</sub>N<sub>5</sub>OS

**2-Amino-4-(furan-3-yl)-6-[(2-hydroxyethyl)sulfanyl]pyridine-3,5-dicarbonitrile (18).** Prepared from **38** according to Procedure A. TLC: SiO<sub>2</sub>, EtOAc/CHX/MeOH 6:3:1; yield 72%; mp 191-192 °C (EtOAc/CHX). <sup>1</sup>H NMR (DMSO-d<sub>6</sub>) 8.26-8.25 (m, 1H, Ar), 7.99 (br s, 2H, NH<sub>2</sub>), 7.92 (t, J= 1.7 Hz, 1H, Ar), 6.88-6.87 (m, 1H, Ar), 4.99 (t, J=5.4 Hz, 1H, OH), 3.64 (q, J=12 Hz, 2H, CH<sub>2</sub>), 3.33 (t, J=6.3 Hz, 2H, CH<sub>2</sub>). Anal. Calc. for C<sub>13</sub>H<sub>10</sub>N<sub>4</sub>O<sub>2</sub>S

**Methyl 3-(((6-amino-3,5-dicyano-4-(furan-3-yl)pyridin-2-yl)thio)methyl)benzoate (19).**

Prepared from **38** according to Procedure A. TLC: SiO<sub>2</sub>, EtOAc/CHX/MeOH 7:2:1; yield 61%; mp 229-231 °C (MeOH/2-methoxyethanol). <sup>1</sup>H NMR (DMSO-d<sub>6</sub>) 8.24 (s, 1H, Ar), 8.09 (s, 1H, Ar), 8.34-7.77 (br s, 2H, NH<sub>2</sub>), 7.90 (t, J=1.7 Hz, 1H, Ar), 7.85 (s, 1H, Ar), 7.83 (s, 1H, Ar), 7.47 (t, J=7.7 Hz, 1H, Ar), 6.87 (d, J=1.8 Hz, 1H, Ar), 4.58 (s, 2H, CH<sub>2</sub>), 3.86 (s, 3H, CH<sub>3</sub>). IR 3373, 3113, 2210, 1527. Anal. Calc. for C<sub>20</sub>H<sub>14</sub>N<sub>4</sub>O<sub>3</sub>S

**2-Amino-6-((2-hydroxyethyl)sulfanyl)-4-(thiophen-2-yl)pyridine-3,5-dicarbonitrile (20).<sup>45</sup>**

Prepared from **39** according to Procedure A. TLC: SiO<sub>2</sub>, EtOAc/CHX/MeOH 6:3:1; yield 76%; mp 154-156 °C (AcOEt/CHX). <sup>1</sup>H NMR (DMSO-d<sub>6</sub>) 8.03 (br s, 2H, NH<sub>2</sub>), 7.94 (d, J=4.9 Hz, 1H, Ar),

7.55 (d, J=3.4 Hz, 1H, Ar), 7.28 (d, J=4 Hz, 1H, Ar), 4.99 (t, J=5.4 Hz, 1H, OH), 3.65 (q, J=12 Hz, 2H, CH<sub>2</sub>), 3.33 (t, J=6.3 Hz, 2H, CH<sub>2</sub>). IR 3320, 3222, 2208. Anal. Calc. for C<sub>13</sub>H<sub>10</sub>N<sub>4</sub>OS<sub>2</sub>.

**2-Amino-6-((2-hydroxyethyl)amino)-4-(thiophen-2-yl)pyridine-3,5-dicarbonitrile (21).**<sup>45</sup>

Prepared from **34** according to Procedure C. Yield 88%; 220-222 °C (EtOH). <sup>1</sup>H NMR (DMSO-d<sub>6</sub>) 7.87 (d, J=4.7 Hz, 1H, Ar), 7.47 (d, J=1.6 Hz, 1H, Ar), 7.42 (br s, 2H, NH<sub>2</sub>), 7.26-7.22 (m, 2H, NH + Ar), 4.74 (t, J=5.1 Hz, 1H, OH), 3.54 (q, J=10.9 Hz, 2H, CH<sub>2</sub>), 3.48 (q, J=10.9, 2H, OCH<sub>2</sub>). IR 3491, 3451, 3338, 2202. Anal. Calc. for C<sub>13</sub>H<sub>11</sub>N<sub>5</sub>OS.

**Methyl 3-(((6-amino-3,5-dicyano-4-(thiophen-2-yl)pyridin-2-yl)sulfanyl)methyl)benzoate (22).**

Prepared from **39** according to Procedure A. TLC: SiO<sub>2</sub>, EtOAc/CHX/MeOH 7:2:1; yield 76%; mp 199-201 °C (EtOH). <sup>1</sup>H NMR (DMSO-d<sub>6</sub>) 8.10 (s, 1H, Ar), 7.94 (d, J=5.0 Hz, 1H, Ar), 8.55-7.72 (m, 2H, NH<sub>2</sub>), 7.86 (s, 1H, Ar), 7.84 (s, 1H, Ar), 7.56 (d, J=2.7 Hz, 1H, Ar), 7.47 (t, J=7.7 Hz, 1H, Ar), 7.27 (dd, J=4.9, 3.8 Hz, 1H, Ar), 4.59 (s, 2H, CH<sub>2</sub>), 3.86 (s, 3H, CH<sub>3</sub>). IR 3462, 3329, 3217, 2210, 1547. Anal. Calc. for C<sub>20</sub>H<sub>14</sub>N<sub>4</sub>O<sub>2</sub>S<sub>2</sub>

**2-Amino-6-((2-hydroxyethyl)sulfanyl)-4-(thiophen-3-yl)pyridine-3,5-dicarbonitrile (23).**

Prepared from **40** according to Procedure A. TLC: SiO<sub>2</sub>, EtOAc/CHX/MeOH 6:3:1; yield 60%; mp 175-178 °C (EtOAc/CHX). <sup>1</sup>H NMR (DMSO-d<sub>6</sub>) 8.03 (q, 1H, J=2.9 Hz, Ar), 7.95 (br s, 2H, NH<sub>2</sub>), 7.76 (q, J=5.0 Hz, 1H, Ar), 7.38 (dd, J=1.3 Hz, 5.0 Hz, 1H, Ar), 5.00 (br s, 1H, OH), 3.65 (t, J=6.4 Hz, 2H, CH<sub>2</sub>), 3.34 (t, J=6.4 Hz, 2H, CH<sub>2</sub>). IR 3320, 3209, 2212. Anal. Calc. for C<sub>13</sub>H<sub>10</sub>N<sub>4</sub>OS<sub>2</sub>.

**2'-Amino-6'-((2-hydroxyethyl)sulfanyl)-3,4'-bipyridine-3',5'-dicarbonitrile (24).** Prepared from

**41** according to Procedure A. TLC: SiO<sub>2</sub>, EtOAc/CHX/MeOH 6:3:1; yield 98%; mp 233-235 °C (EtOAc/CHX). <sup>1</sup>H NMR (DMSO-d<sub>6</sub>) 8.81-8.51 (m, 1H, Ar), 8.10 (br s, 2H, NH<sub>2</sub>), 8.04-8.01 (m, 2H, ar), 7.63-7.52 (m, 1H, Ar), 5.01 (t, J=5.2 Hz, 1H, OH), 3.67 (q, J= 11.5 Hz, 2H, CH<sub>2</sub>), 3.36 (t, J=6.3 Hz, 2H, CH<sub>2</sub>). IR 3319, 3124, 2212. Anal. Calc. for C<sub>14</sub>H<sub>11</sub>N<sub>5</sub>OS.

**2-Amino-6-((2-hydroxyethyl)amino)-4-(pyridin-3-yl)pyridine-3,5-dicarbonitrile (25).** Prepared

from **36** according to Procedure C. Yield 79%; mp 251-253 °C (EtOH). <sup>1</sup>H NMR (DMSO-d<sub>6</sub>): 8.74 (d, J=4.1, Hz 1H, Ar), 8.69 (s, 1H, Ar), 7.96 (d, J=7.9 Hz, 1H, Ar), 7.61-7.58 (m, 1H, Ar), 7.60-7.40

(br s, 2H, NH<sub>2</sub>), 7.33 (t, J=5.2 Hz, 1H, NH), 4.74 (t, J=5.1 Hz, 1H, OH), 3.57-3.54 (m, 2H, CH<sub>2</sub>), 3.51-3.48 (m, 2H, CH<sub>2</sub>). IR 3306, 2206, 1633, 1099, 1026. Anal. Calc. for C<sub>14</sub>H<sub>12</sub>N<sub>6</sub>O

**Methyl 3-(((6'-amino-3',5'-dicyano-(3,4'-bipyridin)-2'-yl)thio)methyl)benzoate (26).** Prepared from **41** according to Procedure A. TLC: SiO<sub>2</sub>, EtOAc/CHX/MeOH 7:2:1; yield 21%; mp 222-224 °C (2-methoxyethanol/EtOH); <sup>1</sup>H NMR (DMSO-d<sub>6</sub>) 8.83-8.67 (m, 2H, Ar), 8.23 (br s, 2H, NH<sub>2</sub>), 8.11 (s, 1H, Ar), 8.03 (d, J=7.9 Hz, 1H, Ar), 7.86 (t, J = 7.8 Hz, 2H, Ar), 7.61 (dd, J=7.7, 4.9 Hz, 1H, Ar), 7.48 (t, J=7.7 Hz, 1H, Ar), 4.61 (s, 2H, CH<sub>2</sub>), 3.86 (s, 3H, CH<sub>3</sub>); <sup>13</sup>C NMR (100 MHz, DMSO-d<sub>6</sub>): 166.44, 159.88, 155.82, 151.73, 149.01, 139.08, 136.86, 134.89, 130.65, 130.36, 129.29, 128.51, 124.01, 115.48, 93.84, 86.77, 52.65, 33.05. Anal. Calc. for C<sub>21</sub>H<sub>15</sub>N<sub>5</sub>O<sub>2</sub>S

**2-(Cyclopentylamino)-4-(furan-2-yl)-6-((2-hydroxyethyl)sulfanyl)pyridine-3,5-dicarbonitrile (27).** Prepared from **44** according to Procedure E. Yield: 89%; mp 185-187 °C (MeOH). <sup>1</sup>H NMR (DMSO-d<sub>6</sub>) 8.10 (s, 1H, Ar), 7.83 (d, J=6.8 Hz, 1H, NH), 7.36 (d, J=3.5 Hz, 1H, Ar), 6.82 (s, 1H, Ar), 5.03 (t, J=5.3 Hz, 1H, OH), 4.60-4.37 (m, 1H, CH), 3.67 (dd, J=12.1, 6.2 Hz, 2H, OCH<sub>2</sub>), 3.31 (t, J=6.2 Hz, 2H, SCH<sub>2</sub>) 1.96 (dd, J=10.6, 6.4 Hz, 2H, CH<sub>2</sub>), 1.82-1.46 (m, 6H, 3CH<sub>2</sub>); <sup>13</sup>C NMR (DMSO-d<sub>6</sub>) 168.59, 157.83, 145.56, 144.17, 116.73, 116.31, 116.07, 113.23, 89.74, 83.21, 59.98, 53.70, 33.33, 32.26, 24.29. IR 3466, 3348, 2210. Anal. Calc. for C<sub>18</sub>H<sub>18</sub>N<sub>4</sub>O<sub>2</sub>S

**2-(Cyclopropylamino)-4-(furan-2-yl)-6-((2-hydroxyethyl)sulfanyl)pyridine-3,5-dicarbonitrile (28).** Prepared from **44** according to Procedure E. Yield 91%; mp 214-216 °C (MeOH). <sup>1</sup>H NMR (DMSO-d<sub>6</sub>) 8.29 (br s, 1H, NH), 8.10 (s, 1H, Ar), 7.37 (d, J=3.4 Hz, 1H, Ar), 6.84 (s, 1H, Ar), 5.01 (t, J=5.4 Hz, 1H, OH), 3.70 (dd, J=12.1, 6.2 Hz, 2H, OCH<sub>2</sub>), 3.38 (t, J=6.5 Hz, 2H, CH<sub>2</sub>), 2.97-2.84 (m, 1H, CH), 0.80 (m, 2H, CH eq), 0.75-0.61 (m, 2H, CH ax). IR 3491, 3302, 2210. Anal. Calc. for C<sub>16</sub>H<sub>14</sub>N<sub>4</sub>O<sub>2</sub>S

**4-(Furan-2-yl)-2-((2-hydroxyethyl)thiosulfanyl)-6-((4-iodophenyl)amino)pyridine-3,5-dicarbonitrile (29).** Prepared from **44** according to Procedure E. Yield 99%; mp 218-220 °C (acetone). <sup>1</sup>H NMR (DMSO-d<sub>6</sub>) 9.93 (br s, 1H, NH), 8.15 (s, 1H, Ar), 7.72 (d, J=8.5 Hz, 2H, Ar), 7.45 (d, J=3.5 Hz, 1H, Ar), 7.38 (d, J=8.6 Hz, 2H, Ar), 6.96-6.78 (m, 1H, Ar), 4.96 (t, J=5.8 Hz, 1H,

OH), 3.58-3.46 (m, 2H, OCH<sub>2</sub>), 3.16 (t, J=6.1 Hz, 2H, SCH<sub>2</sub>); <sup>13</sup>C NMR (DMSO-d<sub>6</sub>) 178.96, 168.75, 156.80, 145.36, 144.60, 138.22, 137.53, 126.43, 117.20, 115.92, 115.83, 113.36, 92.69, 89.73, 59.82, 33.60. IR 3394, 3296, 2216. Anal. Calc. for C<sub>19</sub>H<sub>13</sub>IN<sub>4</sub>O<sub>2</sub>S

**2-(Benzylamino)-4-(furan-2-yl)-6-((2-hydroxyethyl)sulfanyl)pyridine-3,5-dicarbonitrile (30).**

Prepared from **44** according to Procedure E. Yield 86%; mp: 171-173 °C (MeOH). <sup>1</sup>H NMR (DMSO-d<sub>6</sub>) 8.80 (s, 1H, NH), 8.11 (s, 1H, Ar), 7.40 (d, J=3.5 Hz, 1H, Ar), 7.38-7.29 (m, 4H, Ar), 7.25 (s, 1H, Ar), 6.85 (s, 1H, Ar), 4.98 (t, J=5.4 Hz, 1H, OH), 4.70 (d, J=5.4 Hz, 2H, CH<sub>2</sub>), 3.48 (dd, J=11.6, 5.9 Hz, 2H, OCH<sub>2</sub>), 3.16 (t, J=6.1 Hz, 2H, SCH<sub>2</sub>); <sup>13</sup>C NMR (DMSO-d<sub>6</sub>): 168.81, 158.22, 145.51, 144.02, 139.43, 128.80, 127.35, 116.83, 116.22, 116.08, 113.29, 90.03, 83.13, 59.74, 45.18, 33.42. IR 3344, 2208. Anal. Calc. for C<sub>20</sub>H<sub>16</sub>N<sub>4</sub>O<sub>2</sub>S.

**Synthesis of N-(3,5-dicyano-4-(furan-2-yl)-6-((2-hydroxyethyl)thio)pyridin-2-yl)acetamide (31).**

Sodium hydrogen carbonate (0.53 mmol) and 2-bromoethanol (0.39 mmol) were sequentially added to a stirred solution of compound **46**<sup>54</sup> (0.35 mmol) in anhydrous DMF (1 mL). The reaction mixture was kept at rt for 3h and then water (10 mL) was added affording a light brown solid which was filtered and washed with water (10 mL) and Et<sub>2</sub>O (5 mL). The crude product was purified by preparative TLC on silica gel using EtOAc as eluting system, and then recrystallized. Yield 20%; mp 164-166 °C (MeOH). <sup>1</sup>H NMR (DMSO-d<sub>6</sub>) 11.13 (s, 1H, NH), 8.21 (s, 1H, Ar), 7.53 (d, J=3.6 Hz, 1H, Ar), 6.90 (dd, J=3.6, 1.7 Hz, 1H, Ar), 5.07 (s, 1H, OH), 3.70 (t, J=6.2 Hz, 2H, OCH<sub>2</sub>), 3.42 (t, J=6.2 Hz, 2H, SCH<sub>2</sub>), 2.21 (s, 3H, CH<sub>3</sub>); <sup>13</sup>C NMR (DMSO-d<sub>6</sub>) 169.37, 168.55, 155.12, 144.96, 144.30, 118.22, 115.22, 115.09, 113.76, 113.27, 98.59, 94.79, 59.69, 33.87, 24.06; IR 3321, 2218, 1718. Anal. Calc. for C<sub>15</sub>H<sub>12</sub>N<sub>4</sub>O<sub>3</sub>S.

**Synthesis of 2-amino-4-(furan-3-yl)-6-(phenylsulfanyl)pyridine-3,5-dicarbonitrile (33).**

A solution of 3-furaldehyde (10 mmol), malononitrile (20 mmol) and tetrabutylammonium fluoride hydrate (10% mol) in water (50 mL), was stirred at rt for 20 min. Then, thiophenol (10 mmol) was

added and the mixture was heated at 80 °C for 2 h. After cooling at rt, the water was removed under reduced pressure, the residue dissolved in EtOAc (100 mL) and the resulting solution dried over anhydrous sodium sulfate. After distillation of the solvent, the crude product was triturated with a mixture of Et<sub>2</sub>O/EtOH (10:1), collected by filtration and recrystallized. Yield 22%; mp 204-206 °C (MeOH). <sup>1</sup>H NMR (DMSO-d<sub>6</sub>) 8.29-8.22 (m, 1H, Ar), 7.94-7.93 (m, 1H, Ar), 7.81 (br s, 2H, NH<sub>2</sub>), 7.60-7.59 (m, 2H, Ar), 7.51-7.50 (m, 3H, Ar), 6.91-6.90 (m, 1H, Ar). IR 3328, 3218, 2220. Anal. Calc. for C<sub>17</sub>H<sub>10</sub>N<sub>4</sub>OS

**Synthesis of 2-amino-4-(furan-3-yl)-6-sulfanylpuridine-3,5-dicarbonitrile (38).** To a stirred solution of compound **33** (10 mmol) in anhydrous DMF (1 mL) maintained at rt and under nitrogen atmosphere, an excess of anhydrous sodium sulfide (33 mmol) was added. The reaction mixture was heated at 80 °C for 2 h. Then, 1N HCl (25 mL), followed by 6N HCl, was drop by drop added to obtain a precipitate which was collected by filtration, washed with water (20 ml) and Et<sub>2</sub>O (5 ml), and recrystallized. Yield 92%; mp 260-262 °C (EtOH). <sup>1</sup>H NMR (DMSO-d<sub>6</sub>) 12.97 (br s, 1H, SH), 8.27-8.25 (m, 1H, Ar), 8.00 (br s, 2H, NH<sub>2</sub>), 7.90 (t, J=1.6 Hz, 1H, Ar), 6.85- 6.84 (m, 1H, Ar); IR 3307, 3192, 2216. Anal. Calc. for C<sub>11</sub>H<sub>6</sub>N<sub>4</sub>OS

**Synthesis of 2-amino-4-(furan-2-yl)-6-methoxypuridine-3,5-dicarbonitrile (42).**<sup>52</sup> A solution of sodium methoxide (30.4 mmol) in MeOH (20 mL) was rapidly added to a solution of 2-furaldehyde (20.8 mmol), malononitrile (20.8 mmol) and tetrabutylammonium fluoride hydrate (2.1 mmol) in MeOH (10 mL) at rt. Then, a further amount of malononitrile (20.8 mmol) was added and the mixture was refluxed for 3h. The resulting suspension was filtered over celite pad and the filtrate evaporated under reduced pressure. The crude residue was purified by silica gel column chromatography, CH<sub>2</sub>Cl<sub>2</sub> as eluting system. Yield 27%; mp 205-207 °C (EtOH). <sup>1</sup>H NMR (DMSO-d<sub>6</sub>) 8.09 (s, 1H, Ar), 8.05 (br s, 2H, NH<sub>2</sub>), 7.38 (s, 1H, Ar), 6.83 (s, 1H, Ar), 3.97 (s, 3H, CH<sub>3</sub>); IR 3406, 3345, 3244, 2222. Anal. Calc. for C<sub>12</sub>H<sub>8</sub>N<sub>4</sub>O<sub>2</sub>

**Synthesis of 2-amino-4-(furan-2-yl)-6-hydroxypyridine-3,5-dicarbonitrile (43)<sup>53</sup>**

Compound **42**<sup>52</sup> (1.4 mmol) was suspended in a mixture of glacial acetic acid (4 mL) and concentrated HCl (1 mL), and heated at 100 °C for 2 h. Then, the reaction mixture was cooled at rt affording a precipitate which was collected by filtration, washed with water (20 mL) and Et<sub>2</sub>O (5 mL) and dried in oven at 60 °C. Yield 81%; mp 186-188 °C (EtOH). <sup>1</sup>H NMR (DMSO-d<sub>6</sub>) 11.85 (br s, 1H, OH), 8.08 (d, J=1.1 Hz, 1H, Ar), 7.72 (br s, 2H, NH<sub>2</sub>), 7.36 (d, J=3.6 Hz, 1H, Ar), 6.82 (dd, J=3.6, 1.7 Hz, 1H, Ar); IR 3319, 3199, 2226, 2212. Anal. Calc. for C<sub>11</sub>H<sub>6</sub>N<sub>4</sub>O<sub>2</sub>

**Synthesis of 2-chloro-4-(furan-2-yl)-6-((2-hydroxyethyl)thio)pyridine-3,5-dicarbonitrile (44).**

Isoamylnitrite (9 mmol) was added to a suspension of copper (II) chloride (9 mmol) in anhydrous CH<sub>3</sub>CN (5 mL) under nitrogen atmosphere. The reaction mixture was stirred 20 min at rt. Then, compound **1** (1.5 mmol) was added and the reaction was maintained at rt for a weekend. 1N HCl was added until pH 1 and the resulting mixture was extracted with CH<sub>2</sub>Cl<sub>2</sub> (4 x 25 mL). The collected organic layers were washed with brine (2 x 20 mL) and dried (Na<sub>2</sub>SO<sub>4</sub>). The solvent was removed under reduced pressure and the yellow residue triturated with Et<sub>2</sub>O (2 mL), filtered and recrystallized. Yield 67 %; mp 197-199 °C (EtOH). <sup>1</sup>H NMR (DMSO-d<sub>6</sub>) 8.27 (s, 1H, Ar), 7.66 (d, J=3.6 Hz, 1H, Ar), 6.95 (d, J=3.6 Hz, 1H, Ar), 3.70 (t, J=6.3 Hz, 2H, CH<sub>2</sub>), 3.41 (t, J=6.3 Hz, 2H, CH<sub>2</sub>); IR 2230. Anal. Calc. for C<sub>13</sub>H<sub>8</sub>ClN<sub>3</sub>O<sub>2</sub>S

**Synthesis of N-(3,5-dicyano-4-(furan-2-yl)-6-(phenylsulfanyl)pyridin-2-yl)acetamide (45).**

A solution of compound **32**<sup>46</sup> (0.94 mmol) and anhydrous pyridine (0.23 mmol) in acetic anhydride (2 mL) was refluxed for 28h. After removal of the solvent under reduced pressure, a brown solid was obtained which was purified by silica gel column chromatography, eluting system CHX/EtOAc 7:3.



Yield 41%; mp 213-215 °C (EtOH). <sup>1</sup>H NMR (DMSO-d<sub>6</sub>) 10.82 (s, 1H, NH), 8.23 (d, J=1.2 Hz, 1H, Ar), 7.69-7.62 (m, 2H, Ar), 7.54 (m, J=15.1, 4.6 Hz, 4H, Ar), 6.92 (dd, J=3.7, 1.8 Hz, 1H, Ar), 1.92 (s, 3H, CH<sub>3</sub>); IR 3358, 3147, 2216, 1705. Anal. Calc. for C<sub>19</sub>H<sub>12</sub>N<sub>4</sub>O<sub>2</sub>S

**Synthesis of N-(3,5-dicyano-4-(furan-2-yl)-6-sulfanylpiperidin-2-yl)acetamide (46).**<sup>54</sup> Sodium sulfide (1.2 mmol) was added to a solution of compound **45** (0.36 mmol) in anhydrous DMF (0.5 mL), and the reaction mixture was heated at 80 °C for 3h. Then, 0.1N HCl (25 mL) was added followed by addition of 6N HCl until an abundant precipitate formed. The solid was collected by filtration, washed with water (20 mL) and Et<sub>2</sub>O (5 mL), and used for the next step without any further purification. Yield 98%. <sup>1</sup>H NMR (DMSO-d<sub>6</sub>) 12.99 (s, 1H, SH), 11.25 (br s, 1H, NH), 8.19 (s, 1H, Ar), 7.50 (d, J=3.4 Hz, 1H, Ar), 6.89 (s, 1H, Ar), 2.23 (s, 3H, CH<sub>3</sub>). Anal. Calc. for C<sub>13</sub>H<sub>8</sub>N<sub>4</sub>O<sub>2</sub>S

## Pharmacological assays

**Cell culture and membrane preparation.** Wild type CHO cells and hA<sub>1</sub>, hA<sub>2A</sub>, hA<sub>2B</sub> and hA<sub>3</sub> ARs CHO cells were cultured in Dulbecco's modified Eagle's medium with nutrient mixture F12, containing 10% fetal calf serum, penicillin (100 U/ml), streptomycin (100 µg/ml), l-glutamine (2 mM), geneticine (G418; 0.2 mg/ml) at 37°C in 5% CO<sub>2</sub>/95% air<sup>76</sup>. To obtain membranes, the cells were washed with phosphate-buffered saline and resuspended in ice-cold hypotonic buffer (5 mM Tris HCl, 1 mM EDTA, pH 7.4). The cells were homogenized by using a Polytron, centrifuged for 30 min at 40000 g at 4°C and the resulting membranes were used in binding experiments<sup>76</sup>.

**Saturation binding assays.** [<sup>3</sup>H]DPCPX (0.01 to 10 nM), [<sup>3</sup>H]ZM241385 (0.01 to 10 nM) and [<sup>125</sup>I]AB-MECA (0.01 to 10 nM) were used in the saturation binding experiments as radioligands for hA<sub>1</sub>, hA<sub>2A</sub> and hA<sub>3</sub> ARs, respectively. The radioligands and membranes (50 mg of protein per assay) were incubated at 25°C, 90 min for hA<sub>1</sub>ARs, at 4°C, 60 min for hA<sub>2A</sub>ARs and at 4°C, 120 min for hA<sub>3</sub>ARs.

**Competition binding assays.** The affinity to hA<sub>1</sub>, hA<sub>2A</sub> and hA<sub>3</sub> ARs of the novel compounds was studied. Human A<sub>1</sub> ARs competition experiments were performed incubating [<sup>3</sup>H]-8-cyclopentyl-1,3-dipropylxanthine at 1 nM concentration ([<sup>3</sup>H]-DPCPX, K<sub>D</sub> = 1.12 ± 0.11 nM) with 50 µg of protein/100 µl membranes and various concentrations of the newly synthesized compounds in 50 mM Tris HCl, pH 7.4 at 25°C for 90 min. Non-specific binding was calculated in the presence of 1 µM DPCPX and was minor than 10% of the total binding<sup>76</sup>. Human A<sub>2A</sub> ARs inhibition binding assays were carried out incubating 1 nM of [<sup>3</sup>H]-ZM241385 (K<sub>D</sub> = 1.25 ± 0.13 nM) with membranes (50 µg of protein/100 µl) and the examined compounds at different concentrations at 4°C for 60 min in 50 mM Tris HCl (pH 7.4) with 10 mM of MgCl<sub>2</sub>. The presence of 1 µM ZM241385 was used as a condition to evaluate non-specific binding that was about 20% of the total binding<sup>77</sup>. Human A<sub>3</sub> ARs competition binding experiments were executed incubating 50 µg of protein/100 µl of membranes with 0.5 nM [<sup>125</sup>I]-N<sup>6</sup>-(4-aminobenzyl)-N-methylcarboxamidoadenosine ([<sup>125</sup>I]-ABMECA, K<sub>D</sub> = 0.85 ± 0.07 nM) in the presence of the novel compounds for 120 min at 4°C in 50 mM Tris HCl buffer (pH 7.4), 10 mM MgCl<sub>2</sub>, 1 mM EDTA. The presence of 1 µM ABMECA was utilized to evaluate non-specific binding that was minor than 10% of the total binding<sup>78</sup>. Each in vitro assay includes four independent experiments, each performed in triplicate.

The samples were filtered in a Brandel cell harvester (Brandel Instruments, Unterföhring, Germany) to separate bound and free radioactivity by using Whatman GF/B glass fiber filters. Bound radioactivity was counted by means of a Packard Tri Carb 2810 TR scintillation counter (Perkin Elmer).

**Cyclic AMP assays.** Wild type CHO cells and CHO cells transfected with hA<sub>1</sub>, hA<sub>2A</sub> and hA<sub>2B</sub> ARs were washed with phosphate-buffered saline, trypsinized and centrifuged at 200 g for 10 min. Cells were plated in 96-well white half-area microplate (Perkin Elmer, Boston, USA) in a buffer Hank Balanced Salt Solution containing 5 mM HEPES, 0.5 mM Ro 20-1724, 0.1% BSA, 1 IU/ml adenosine deaminase. The novel compounds at the final concentrations from 1 nM to 1 µM were tested alone and/or in the presence of CCPA 1 nM (for hA<sub>1</sub>AR), CGS 21680 10 nM (for hA<sub>2A</sub>AR) or NECA 100

nM (for hA<sub>2B</sub>AR). AlphaScreen cAMP Detection Kit (Perkin Elmer, Boston, USA) was used to quantified cAMP levels following the manufacturer's instructions<sup>79</sup>. Perkin Elmer EnSight Multimode Plate Reader was used to read the plates. Each in vitro assay includes four independent experiments, each performed in triplicate.

**Data Analysis.** A Bio-Rad method with bovine albumin as a standard reference was used to the evaluation of the protein concentration. From the IC<sub>50</sub> values obtained in competition binding experiments, inhibitory binding constant (K<sub>i</sub>) values were evaluated using the Cheng & Prusoff equation  $K_i = IC_{50} / (1 + [C^*] / K_D^*)$ , where [C\*] is the radioligand concentration and K<sub>D</sub>\* its dissociation constant.<sup>78</sup> Affinity (K<sub>i</sub>) and potency (IC<sub>50</sub>) values were obtained by non-linear regression analysis using the equation for a sigmoid concentration-response curve (Graph-PAD Prism, San Diego, CA, U.S.A).

**Animals.** Male CD-1 albino mice (Envigo, Varese, Italy) weighing approximately 22–25 g (three months of age) at the beginning of the experimental procedure, were used. Animals were housed in CeSAL (Centro Stabulazione Animali da Laboratorio, University of Florence) and used at least 1 week after their arrival. Ten mice were housed per cage (size 26 × 41 cm); animals were fed a standard laboratory diet and tap water *ad libitum*, and kept at 23 ± 1 °C with a 12 h light/dark cycle, light at 7 a.m. All animal manipulations were carried out according to the Directive 2010/63/EU of the European parliament and of the European Union council (22 September 2010) on the protection of animals used for scientific purposes. The ethical policy of the University of Florence complies with the Guide for the Care and Use of Laboratory Animals of the US National Institutes of Health (NIH Publication No. 85-23, revised 1996; University of Florence assurance number: A5278-01). Formal approval to conduct the experiments described was obtained from the Animal Subjects Review Board of the University of Florence. Experiments involving animals have been reported according to ARRIVE guidelines.<sup>80</sup> All efforts were made to minimize animal suffering and to reduce the number of animals used.

**Oxaliplatin-induced neuropathic pain model.** Mice treated with oxaliplatin (2.4 mg kg<sup>-1</sup>) were administered i.p. on days 1-2, 5-9, 12-14 (10 i.p. injections) .<sup>81</sup> Oxaliplatin was dissolved in 5% glucose solution. Control animals received an equivalent volume of vehicle. Behavioral tests were performed on day 15.

**Cold Plate Test.** The animals were placed in a stainless steel box (12 cm × 20 cm × 10 cm) with a cold plate as floor. The temperature of the cold plate was kept constant at 4°C ± 1°C. Pain-related behavior (licking of the hind paw) was observed and the time (seconds) of the first sign was recorded. The cut-off time of the latency of paw lifting or licking was set at 60 seconds.<sup>82</sup>

**Compound administrations.** Compound **9-12** were dissolved in 1% CMC and orally administered. Measurements were performed 15, 30, 45, 60 and 75 min after injection. Control mice were treated with vehicle. The non-selective nAChR antagonist mecamylamine (meca; 2 mg kg<sup>-1</sup> i.p.) and the selective alpha7 nAChR antagonist methyllycaconitine (MLA; 6 mg kg<sup>-1</sup> i.p.) were administered 15 min before tested compounds. Measurements were performed 15, 30, 45, and 60 min after the injection of tested compounds. Control mice were treated with vehicle.

**Statistical analysis.** Behavioural measurements were performed on 10 mice for each treatment carried out in 2 different experimental sets. Results were expressed as mean ± S.E.M. The analysis of variance of behavioural data was performed by one way ANOVA, a Bonferroni's significant difference procedure was used as post-hoc comparison. *P* values of less than 0.05 or 0.01 were considered significant. Investigators were blind to all experimental procedures. Data were analyzed using the “Origin 9” software (OriginLab, Northampton, USA).

## Molecular modelling

Receptor refinement and energy minimization tasks were carried out using Molecular Operating Environment (MOE, version 2014.09) suite.<sup>57</sup> Docking experiments were performed with CCDC Gold<sup>58</sup> and Autodock (within PyRx interface) .<sup>59-61</sup> All ligand structures were optimized using

RHF/AM1 semi-empirical calculations and the software package MOPAC<sup>83</sup> implemented in MOE was utilized for these calculations.

**A<sub>1</sub>AR and A<sub>2A</sub>AR crystal structures refinement.** The recently published crystal structure of the human A<sub>1</sub>AR and the crystal structure of the human A<sub>2A</sub>AR in complex with the covalently bound ligand DU172 and inverse agonist ZM241385, respectively, were downloaded by the Protein Data Bank webpage (<http://www.rcsb.org>; pdb code: 5UEN; 3.2-Å resolution<sup>56</sup> and pdb code: 4EIY; 1.8-Å resolution,<sup>62</sup> respectively). The A<sub>1</sub>AR was then rebuilt by removing the covalently bound ligand DU172 and the engineered segment bRIL and by restoring the IL3 missing loop and the wild type receptor sequence that was changed with the Asn159Ala mutation inserted in the X-ray structure. The Homology Modeling tool of MOE was used for these tasks. The A<sub>2A</sub>AR crystal structure was used in its original form to which all hydrogen atoms were added within MOE. The protein structures were then energetically minimized with MOE using the AMBER99 force field until the RMS gradient of the potential energy was less than 0.05 kJ mol<sup>-1</sup> Å<sup>-1</sup>. Reliability and quality of the models were checked using the Protein Geometry Monitor application within MOE, which provides a variety of stereo-chemical measurements for inspection of the structural quality in a given protein, like backbone bond lengths, angles and dihedrals, Ramachandran  $\phi$ - $\psi$  dihedral plots, and sidechain-rotamer and non-bonded contact quality.

**Homology modeling of the human A<sub>3</sub>AR structure.** A homology model of the human A<sub>3</sub>AR was built using the above cited X-ray structure of the antagonist-bound A<sub>1</sub>AR as templates (pdb code: 5UEN)<sup>34</sup>. A multiple alignment of the AR primary sequences was built within MOE as preliminary step. The Homology Modelling tool of MOE was employed even for this task. The obtained A<sub>3</sub>AR model was then energetically minimized with the same protocol of the other receptors (see above).

**Molecular docking analysis.** Docking analyses were performed by using CCDC Gold<sup>58</sup> and Autodock.<sup>59,60</sup> Gold tool was used with default efficiency settings through MOE interface, by selecting ChemScore as scoring function and 50 poses to be generated for each ligand. Autodock 4.2.6 software was used with PyRx<sup>61</sup> interface. Lamarckian genetic algorithm was employed for this

analysis with the following settings: 50 runs for each ligand; 2,500,000 as maximum number of energy evaluations; 27,000 as maximum number of generations; 0.02 as rate of gene mutation and 0.8 as rate of crossover. The grid box was set with 50, 50, and 50 points in the *x*, *y*, and *z* directions, respectively, with the default grid spacing of 0.375 Å.

**Post Docking analysis. Residue interaction analysis.** The interactions between the ligands and the A<sub>1</sub>AR receptors binding site were analyzed by using the *IF-E 6.0* tool retrievable at the SVL exchange service (Chemical Computing Group, Inc. SVL exchange: <http://svl.chemcomp.com>). The program calculates and displays the atomic and residue interaction forces as 3D vectors. It also calculates the per-residue interaction energies, where negative and positive energy values are associated to favorable and unfavorable interactions, respectively. For each A<sub>1</sub>AR structure, a shell of residues contained within a 10 Å distance from ligand were considered for this analysis.

## Stability studies

**Chemicals.** Acetonitrile, ethanol (Chromasolv), formic acid and (MS grade), NaCl, KCl, Na<sub>2</sub>HPO<sub>4</sub> 2H<sub>2</sub>O, KH<sub>2</sub>PO<sub>4</sub> (Reagent grade), 2-[[6-Amino-3,5-dicyano-4-(4-(cyclopropylmethoxy)phenyl)pyridin-2-yl]thio}acetamide (BAY60-6583, used as internal standard), Enalapril and Ketoprofen (analytical standard) were purchased by Sigma-Aldrich (Milan, Italy). Ketoprofen Ethyl Ester (KEE) were obtained by Fisher's reaction from Ketoprofen and ethanol. MilliQ water 18 MΩ was obtained from Millipore's Simplicity system (Milan - Italy). Phosphate buffer solution (PBS) was prepared by adding 8.01 g L<sup>-1</sup> of NaCl, 0.2 g L<sup>-1</sup> of KCl, 1.78 g L<sup>-1</sup> of Na<sub>2</sub>HPO<sub>4</sub> \* 2H<sub>2</sub>O and 0.27 g L<sup>-1</sup> of KH<sub>2</sub>PO<sub>4</sub>. Human plasma was collected from healthy volunteer and was kept at -80 °C until use. Sprague Dawley male rat plasma was heparinized, filtered and kept at -80 °C until use.

**Instrumental.** The LC-MS/MS analysis was carried out using a Varian 1200L triple quadrupole system (Palo Alto, CA, USA) equipped by two Prostar 210 pumps, a Prostar 410 autosampler and an Elettrospray Source (ESI) operating in negative ions. The ion sources and ion optics parameters were

1  
2  
3  
4  
5  
6  
7  
8  
9  
10  
11  
12  
13  
14  
15  
16  
17  
18  
19  
20  
21  
22  
23  
24  
25  
26  
27  
28  
29  
30  
31  
32  
33  
34  
35  
36  
37  
38  
39  
40  
41  
42  
43  
44  
45  
46  
47  
48  
49  
50  
51  
52  
53  
54  
55  
56  
57  
58  
59  
60

optimized during the calibration of the instrument introducing, via syringe pump at 10  $\mu\text{L min}^{-1}$ , a 1  $\mu\text{g mL}^{-1}$  tuning solution.

Raw-data were collected and processed by Varian Workstation Vers. 6.8 software.

G-Therm 015 thermostatic oven was used to maintained the samples at 37  $^{\circ}\text{C}$  during the stability test.

**Method LC-MS/MS.** The chromatographic parameters employed to analyse the samples were tuned to minimize the run time and were reported as follows:

- column, Pursuit XRs C18 length = 30 mm internal diameter= 2mm; particle size = 3  $\mu\text{m}$  purchased from Agilent Technologies (Palo Alto, CA, USA)
- acidic mobile phase, composed by 10mM of formic acid solution (solvent A) and 10 mM of formic acid in acetonitrile (solvent B).
- flow rate and the injection volume were 0.25  $\text{mL min}^{-1}$  and 5  $\mu\text{L}$  respectively.

The elution gradient is shown in Table 6.

The analyses were acquired in Multiple Reaction Monitoring (MRM), parameters are reported in Table 7, using 100 ms of dwell time and argon at 2.0 mTorr as collision gas.

**Table 6.** Elution gradient of mobile phase used for LC-MS/MS analyses.

Time (min)	A (%)
0.00	90
4.00	10
6.00	10
6.01	90
8.00	90

**Table 7.** MRM parameters.

Compd	Precursor Ion (m/z)	Quantifier Ion (m/z) [collision energy (V)]	Qualifier Ion (m/z) [collision energy (V)]
<b>10</b>	389	209 [25]	362 [15]
BAY60-6583	378	304 [20]	249 [30]
KEE	283	209 [10]	105 [25]
Enalapril	377	234 [15]	303 [15]

**Standard solutions and calibration curves.** Stock solutions of analyte and internal standard (ISTD) were prepared in acetonitrile at 1.0 mg mL<sup>-1</sup> and stored at 4 °C. Working solutions of analyte were freshly prepared by diluting stock solution up to a concentration of 10 µM and 1 µM (Working solution 1 and 2 respectively) in mixture of mQ water/acetonitrile 80:20 (v/v). The ISTD working solution was prepared in acetonitrile at 25 ng mL<sup>-1</sup> (ISTD solution).

A six levels calibration curve was prepared by adding proper volumes of working solution 1 or 2 to a constant volume of ISTD solution (300 µL corresponding to 7.5 ng of ISTD). The obtained solutions were dried under a gentle nitrogen stream and dissolved in 1.5 mL of mQ water/acetonitrile 80:20 (v/v) added with 10 mM of formic acid. Final concentrations of calibration levels were: 0; 0.10; 0.20; 0.50; 0.75 and 1.00 µM.

All calibration levels were analyzed six times by LC-MS/MS method.

**Sample preparation.** Each sample was prepared adding 10 µL of Working solution 1 to 100 µL of PBS or plasma. The obtained solutions correspond to 1 µM of analyte.

Each set of samples was incubated in triplicate at four different times, 0, 30, 60 and 120 min. at 37°C. Therefore, the degradation profile of analyte was represented by a batch of 12 samples (4 incubation times x 3 replicates). After the incubation, the samples were added with 300 µL of ISTD solution and



1  
2  
3  
4  
5  
6  
7  
8  
9  
10  
11  
12  
13  
14  
15  
16  
17  
18  
19  
20  
21  
22  
23  
24  
25  
26  
27  
28  
29  
30  
31  
32  
33  
34  
35  
36  
37  
38  
39  
40  
41  
42  
43  
44  
45  
46  
47  
48  
49  
50  
51  
52  
53  
54  
55  
56  
57  
58  
59  
60

centrifuged. The supernatants were transferred in autosampler vials and dried under a gentle stream of nitrogen.

The dried samples were dissolved in 1.5 mL of mQ water/acetonitrile 80:20 added with 10 mM of formic acid. The obtained sample solutions were analysed by LC-MS/MS method described above.

**Linearity and LOD.** Calibration curve of analyte was obtained by plotting the peak area ratios (PAR), between quantitation ions of analyte and ISTD, versus the nominal concentration of the calibration solution. A linear regression analysis was applied to obtain the best fitting function between the calibration points.

The precision was evaluated through the relative standard deviation (RSD%) of the quantitative data of the replicate analysis of highest level of calibration curve.

In order to obtain reliable LOD values, the standard deviation of response and slope approach was employed.<sup>84</sup> The estimated standard deviations of responses were obtained by the standard deviation of y-intercepts (SDY-I) of regression lines. The obtained linear regressions, the linearity coefficients, precision and the estimated LOD values for the analyte are reported in Table 8.

**Table 8.** Linear regressions data, linearity coefficient, precision and LOD value.

Compd	Slope (PAR/ $\mu$ M)	Intercept (PAR)	R <sup>2</sup>	Precision RSD	LOD ( $\mu$ M)
10	0.805	0.045	0.992	3.5%	0.10

**ASSOCIATED CONTENT**

**Supporting Information**

- Combustion analysis data of the newly synthesized compounds and chemical degradation profiles of compound **10**, Ketoprofen Ethyl Ester (KEE) and Enalapril in different matrices. (PDF)

- PDB coordinates of the 3D structure of the hA<sub>2A</sub>AR (PDB code 4EIY) that were added of hydrogen atoms and missing loop segments and energetically minimized. (PDB)
- PDB coordinates of the 3D structure of the hA<sub>1</sub>AR (PDB code 5UEN) that were added of hydrogen atoms and missing loop segments and energetically minimized. (PDB)
- PDB coordinates of the homology model of the hA<sub>3</sub> adenosine receptor based on the hA<sub>1</sub> receptor X-ray structure (PDB code 5UEN) as a template. (PDB)
- Molecular formula strings. (CSV)

## AUTHOR INFORMATION

### Corresponding author

\*Tel: +39 055 4573722. e-mail: daniela.catarzi@unifi.it.

### ORCID

Daniela Catarzi [0000-0002-8821-928X](https://orcid.org/0000-0002-8821-928X)

### Notes

The authors declare no competing financial interest.

**ACKNOWLEDGMENTS.** The work was financially supported by the Italian Ministry for University and Research (MIUR, PRIN 2010-2011, 20103W4779\_004 project) and intramural Grant from the University of Florence (ex 60%).

### ABBREVIATIONS USED

ABMECA, N<sup>6</sup>-(4-aminobenzyl)-N-methylcarboxamidoadenosine; Ado, Adenosine; AR, adenosine receptor; CCPA, 2-chloro-N<sup>6</sup>-cyclopentyladenosine; CHO, Chinese Hamster Ovary; CPA, N<sup>6</sup>-cyclopentyladenosine; DPCPX, 8-cyclopentyl-1,3-dipropylxanthine; EL, extracellular loop; HEPES, 4-(2-hydroxyethyl)-1-piperazineethanesulfonic acid; KEE, Ketoprofen Ethyl Ester; meca, mecamlamine; MLA, methyllycaconitine; MOE, molecular operating environment; nAChR, nicotinic acetylcholine receptor; NECA, 5'-(N-ethyl-carboxamido)adenosine; RMS, root-mean-square; TM, transmembrane.

## References

1. Borea, P. A.; Gessi, S.; Merighi, S.; Varani, K. Adenosine as a multisignalling guardian angel in human diseases: when, where and how does it exert its protective effects? *Trends Pharmacol. Sci.* **2016**, *37*, 419–434.
2. Borea, P. A.; Gessi, S.; Merighi, S.; Vincenzi, F.; Varani, K. Pharmacology of adenosine receptors: the state of the art. *Physiol. Rev.* **2018**, *98*, 1591-1625.
3. Chen, J. F.; Eltzschig, H. K.; Fredholm, B. B. Adenosine receptors as drug targets – what are the challenges? *Nature Rev. Drug Discovery* **2013**, *12*, 265-286.
4. Stone, T. W.; Ceruti, S.; Abbracchio, M. P. Adenosine receptors and neurological disease: neuroprotection and neurodegeneration. *Handb. Exp. Pharmacol.* **2009**, *193*, 535-587.
5. Gomes, C. V.; Kaster, M. P.; Tomé, A. R.; Agostinho, P. M.; Cunha, R. A. Adenosine receptors and brain diseases: neuroprotection and neurodegeneration. *Biochim. Biophys. Acta* **2011**, *1808*, 1380-1399.
6. Müller, C. E.; Jacobson, K. A. Recent developments in adenosine receptor ligands and their potential as novel drugs. *Biochim. Biophys. Acta* **2011**, *1808*, 1290-1308.
7. Evans-Molina, C. Adenosine and seizures - What's the big fat deal? *Sci. Transl. Med.* **2011**, *3*, 92-113.
8. Rebola, N.; Simões, A. P.; Canas, P. M.; Tomé, A. R.; Andrade, G. M.; Barry, C. E.; Agostinho, P. M.; Lynch, M. A.; Cunha, R. A. Adenosine A<sub>2A</sub> receptors control neuroinflammation and consequent hippocampal neuronal dysfunction. *J. Neurochem.* **2011**, *117*, 100-111.
9. Pinna, A.; Pontis, S.; Borsini, F.; Morelli, M. Adenosine A<sub>2A</sub> receptor antagonists improve deficits in initiation of movement and sensory motor integration in the unilateral 6-hydroxydopamine rat model of Parkinson's disease. *Synapse* **2007**, *61*, 606–614.
10. Horiuchi, H.; Ogata, T.; Morino, T.; Yamamoto, H. Adenosine A<sub>1</sub> receptor agonists reduce hyperalgesia after spinal cord injury in rats. *Spinal Cord* **2010**, *48*, 685-690.
11. Sawynok, J. Adenosine receptor targets for pain. *Neuroscience* **2016**, *338*, 1-18.

12. Rivera-Oliver, M.; Díaz-Ríos, M. Using caffeine and other adenosine receptor antagonists and agonists as therapeutic tools against neurodegenerative diseases: A review. *Life Sci.* **2014**, *101*, 1-9.
13. Bilkei-Gorzo, A.; Abo-Salem, O. M.; Hayallah, A. M.; Michel, K.; Müller, C. E.; Zimmer, A. Adenosine receptor subtype-selective antagonists in inflammation and hyperalgesia. *Naunyn Schmiedebergs Arch. Pharmacol.* **2008**, *377*, 65-76.
14. Pechlivanova, D. M.; Georgiev, V. P. Effects of single and long-term theophylline treatment on the threshold of mechanical nociception: contribution of adenosine A<sub>1</sub> and  $\alpha$ 2-adrenoceptors. *Methods Find. Exp. Clin. Pharmacol.* **2005**, *27*, 659-664.
15. Gong, Q. J.; Li, Y. Y.; Xin, W. J.; Wei, X. H.; Cui, Y. Wang. J.; Liu, Y.; Liu, C. C.; Li, Y. Y.; Liu, X. G. Differential effects of adenosine A<sub>1</sub> receptor on pain-related behavior in normal and nerve injured rats. *Brain Res.* **2010**, *1361*, 23-30.
16. Katz, N. K.; Ryals, J. M.; Wright, D. E. Central or peripheral delivery of an adenosine A<sub>1</sub> receptor agonist improves mechanical allodynia in mouse model of painful diabetic neuropathy. *Neuroscience*, **2015**, *285*, 312-323.
17. Ferré, S.; Diamond, I.; Goldberg, S. R.; Yao, L.; Hourani, S. M. O.; Huang, Z. L.; Urade, Y.; Kitchen, I. Adenosine A<sub>2A</sub> receptor in ventral striatum, hypothalamus and nociceptive circuitry. Implication for drug addiction, sleep and pain. *Prog. Neurobiol.* **2007**, *83*, 332-347.
18. Cunha, R. A. Neuroprotection by adenosine in the brain: from A<sub>1</sub> receptor activation to A<sub>2A</sub> receptor blockade. *Purinergic Signal.* **2005**, *1*, 111-134.
19. Stockwell, J.; Jakova, E.; Cayabyab, F. S. Adenosine A<sub>1</sub> and A<sub>2A</sub> receptor in the brain: current research and their role in neurodegeneration. *Molecules* **2017**, *22*, 676.
20. Dunwiddie, T. V.; Haas, H. L.; Adenosine increases synaptic facilitation in the in vitro rat hippocampus: evidence for a presynaptic site of action. *J. Physiol.* **1985**, *369*, 365-377.
21. Alnouri, M. W.; Jepards, S.; Casari, A.; Schiedel, A. C.; Hinz, S.; Müller, C. E. Selectivity is species-dependent: characterization of standard agonists and antagonists at human, rat, and mouse adenosine receptors. *Purinergic Signal.* **2015**, *11*, 389-407.

22. Galeotti, N.; Ghelardini, C.; Grazioli, I.; Uslenghi, C. Indomethacin, caffeine and prochlorperazine alone and combined revert hyperalgesia in vivo models of migraine. *Pharmacol. Res.* **2002**, *46*, 245-250.
23. Wu, W. P.; Hao, J. X.; Fredholm, B. B.; Wiesenfeld-Hallin, Z.; Xu, X. J. Effect of acute and chronic administration of caffeine on pain-like behaviors in rats with partial sciatic nerve injury. *Neurosci. Lett.* **2006**, *402*, 164-166.
24. Sawynok, J. Caffeine and pain. *Pain* **2011**, *152*, 726-729.
25. Scott, J. R.; Hassett, A. L.; Brummett, C. M.; Harris, R. E.; Clauw, D. J.; Harte, S. E. Caffeine as an opioid analgesic adjuvant in fibromyalgia. *J. Pain Res.* **2017**, *10*, 1801-1809.
26. Poli, D.; Catarzi, D.; Colotta, V.; Varano, F.; Filacchioni, G.; Daniele, S.; Trincavelli, L.; Martini, C.; Paoletta, S.; Moro, S. The identification of the 2-phenylphthalazin-1(2H)-one scaffold as a new decorable core skeleton for the design of potent and selective human A<sub>3</sub> adenosine receptor antagonists. *J. Med. Chem.* **2011**, *54*, 2102-2113.
27. Squarcialupi, L.; Colotta, V.; Catarzi, D.; Varano, F.; Filacchioni, G.; Varani, K.; Corciulo, C.; Vincenzi, F.; Borea, P. A.; Ghelardini, C.; Di Cesare Mannelli, L.; Ciancetta, A.; Moro, S. 2-Arylpyrazolo[4,3- d]pyrimidin-7-amino derivatives as new potent and selective human A<sub>3</sub> adenosine receptor antagonists. Molecular modeling studies and pharmacological evaluation. *J. Med. Chem.* **2013**, *56*, 2256-2269.
28. Squarcialupi, L.; Colotta, V.; Catarzi, D.; Varano, F.; Betti, M.; Varani, K.; Vincenzi, F.; Borea, P. A.; Porta, N.; Ciancetta, A.; Moro, S. 7- Amino-2-phenylpyrazolo[4,3-d]pyrimidine derivatives: Structural investigations at the 5-position to target human A<sub>1</sub> and A<sub>2A</sub> adenosine receptors. Molecular modeling and pharmacological studies. *Eur. J. Med. Chem.* **2014**, *84*, 614-627.
29. Varano, F.; Catarzi, D.; Squarcialupi, L.; Betti, M.; Vincenzi, F.; Ravani, A.; Varani, K.; Dal Ben, D.; Thomas, A.; Volpini, R.; Colotta, V. Exploring the 7-oxo-thiazolo[5,4-d]pyrimidine core for the design of new human adenosine A<sub>3</sub> receptor antagonists. Synthesis, molecular modeling studies and pharmacological evaluation. *Eur. J. Med. Chem.* **2015**, *96*, 105-121.

30. Catarzi, D.; Varano, F.; Poli, D.; Squarcialupi, L.; Betti, M.; Trincavelli, L.; Martini, C.; Dal Ben, D.; Thomas, A.; Volpini, R.; Colotta, V. 1,2,4-Triazolo[1,5-a]quinoxaline derivatives and their simplified analogues as adenosine A<sub>3</sub> receptor antagonists. Synthesis, structure–affinity relationships and molecular modeling studies. *Bioorg. Med. Chem.* **2015**, *23*, 9–21.
31. Squarcialupi, L.; Catarzi, D.; Varano, F.; Betti, M.; Falsini, M.; Vincenzi, F.; Ravani, A.; Ciancetta, A.; Varani, K.; Moro, S.; Colotta, V. Structural refinement of pyrazolo[4,3-d]pyrimidine derivative to obtain highly potent and selective antagonists for the human A<sub>3</sub> adenosine receptor. *Eur. J. Med. Chem.* **2016**, *108*, 117–133.
32. Varano, F.; Catarzi, D.; Vincenzi, F.; Betti, M.; Falsini, M.; Ravani, A.; Borea, P. A.; Colotta, V.; Varani, K. Design, synthesis, and pharmacological characterization of 2-(2-furanyl)thiazolo[5,4-d]pyrimidine-5,7-diamine derivatives: New highly potent A<sub>2A</sub> adenosine receptor inverse agonists with antinociceptive activity. *J. Med. Chem.* **2016**, *59*, 10564–10576.
33. Poli, D.; Falsini, M.; Varano, F.; Betti, M.; Varani, K.; Vincenzi, F.; Pugliese, A. M.; Pedata, F.; Dal Ben, D.; Thomas, A.; Palchetti, I.; Bettazzi, F.; Catarzi, D.; Colotta, V. Imidazo[1,2-a]pyrazin-8-amine core for the design of new adenosine receptor antagonists: Structural exploration to target the A<sub>3</sub> and A<sub>2A</sub> subtypes. *Eur. J. Med. Chem.* **2017**, *125*, 611–628.
34. Falsini, M.; Squarcialupi, L.; Catarzi, D.; Varano, F.; Betti, M.; Dal Ben, D.; Marucci, G.; Buccioni, M.; Volpini, R.; De Vita, T.; Cavalli, A.; Colotta, V. The 1,2,4-Triazolo[4,3-a]pyrazin-3-one as a versatile scaffold for the design of potent adenosine human receptor antagonists. Structural investigations to target the A<sub>2A</sub> receptor subtype. *J. Med. Chem.* **2017**, *60*, 5772–5790.
35. Varano, F.; Catarzi, D.; Vincenzi, F.; Falsini, M.; Pasquini, S.; Borea, P. A.; Colotta, V.; Varani, K. Structure-activity relationship studies and pharmacological characterization of N5-heteroarylalkyl-substituted-2-(2-furanyl) thiazolo[5,4-d]pyrimidine-5,7-diamine-based derivatives as inverse agonists at human A<sub>2A</sub> adenosine receptor. *Eur. J. Med. Chem.* **2018**, *155*, 552–561.

36. Catarzi, D.; Varano, F.; Falsini, M.; Varani, K.; Vincenzi, F.; Pasquini, S.; Dal Ben, D.; Colotta, V. Development of novel pyridazinone-based adenosine receptor ligands. *Bioorg. Med. Chem.* **2018**, *28*, 1484–1489.
37. Betti, M.; Catarzi, D.; Varano, F.; Falsini, M.; Varani, K.; Vincenzi, F.; Dal Ben, D.; Lambertucci, C.; Colotta, V. The aminopyridine-3,5-dicarbonitrile core for the design of new non-nucleoside-like agonists of the human adenosine A<sub>2B</sub> receptor. *Eur. J. Med. Chem.* **2018**, *150*, 127-139
38. Beukers, M. W.; Chang, L. C. W.; von Frijtag Drabbe Kunzel, J. K.; Mulder-Krieger, T.; Spanjersberg, R. F.; Brussee, J.; IJzerman, A. P. New, non-adenosine, high-potency agonists for the human adenosine A<sub>2B</sub> receptor with an improved selectivity profile compared to the reference agonist N-ethylcarboxamidoadenosine. *J. Med. Chem.* **2004**, *47*, 3707–3079.
39. Chang, L. C. W.; von Frijtag Drabbe Künzel, J. K.; Mulder-Krieger, T.; Spanjersberg, R. F.; Roerink, S. F.; van den Hout, G.; Beukers, M. W.; Brussee, J.; IJzerman, A. P. A series of ligand displaying a remarkable agonistic-antagonistic profile at the adenosine A<sub>1</sub> receptor. *J. Med. Chem.* **2005**, *48*, 2045-2053.
40. Meibom, D.; Albrecht-Küpper, B.; Diedrichs, N.; Hübsch, W.; Kast, R.; Krämer, T.; Krenz, U.; Lerchen, H.-J.; Mittendorf, J.; nell, P. G.; Süssmeier, F.; Vakalopoulos, A.; Zimmermann, K. neladenoson bialanate hydrochloride: a prodrug of a partial adenosine A<sub>1</sub> receptor agonist for the chronic treatment of heart disease. *ChemMedChem* **2017**, *12*, 728-737.
41. Thimm, D.; Schiedel, A. C.; Sherbiny, F. F.; Hinz, S.; Hochheiser, K.; Bertarelli, D. C. G.; Maaß, A.; Müller, C. E. Ligand-specific binding and activation of the human adenosine A<sub>2B</sub> receptor. *Biochemistry* **2013**, *52*, 726–740.
42. Dal Ben, D.; Buccioni, M.; Lambertucci, C.; Thomas, A.; Volpini, R. Simulation and comparative analysis of binding modes of nucleoside and non-nucleoside agonists at the A<sub>2B</sub> adenosine receptor. *In Silico Pharmacol.* **2013**, *1*, 24.

43. Krivokolyko, S. G.; Dyachenko, V. D. Esters and nitriles of 3-phenylacrylic and 3-(2-furyl)acrylic acid in synthesis of 6-amino-3,5-dicyano-4-phenyl(or 2-furyl)pyridine-2(1H)-thiones and – selenones. *Ukrainskii Khimicheskii Zhurnal* **1996**, *62*, 61-66.
44. May, B. C. H.; Zorn, J. A.; Witkop, J.; Sherrill, J.; Wallace, A. C.; Legname, G.; Prusiner, S. B.; Cohen, F. E.; Structure-activity relationship study of prion inhibition by 2-aminopyridine-3,5-dicarbonitrile-based compounds: parallel synthesis, bioactivity, and in vitro pharmacokinetics. *J. Med. Chem.* **2007**, *50*, 65-73.
45. Harada, H.; Watanuki, S.; Takuwa, T.; Kawaguchi, K.; Okazaki, T.; Hirano, Y.; Saitoh, C. Preparation of Dicyanopyridine Derivatives as High-Conductance Calcium-Sensitive Potassium Channel Openers. WO patent 06237 (A1), Jan 24, 2002.
46. Sridhar, M.; Ramanaiah, B. C.; Narsaiah, C.; Mahesh, B.; Kumaraswamy, M.; Mallu, K. K. R.; Ankathi, V. M.; Shanthan Rao, P. Novel ZnCl<sub>2</sub>-catalyzed one-pot multicomponent synthesis of 2-amino-3,5-dicarbonitrile-6-thio-pyridines. *Tetrahedron Lett.* **2009**, *50*, 3897-3900.
47. Evdokimov, N. M.; Kireev, A. S.; Yakovenko, A. A.; Antipin, M. Y.; Magedov, I. V.; Kornienko, A. One-step synthesis of heterocyclic privileged medicinal scaffolds by a multicomponent reaction of malononitrile with aldehydes and thiols. *J. Org. Chem.* **2007**, *72*, 3443-3453.
48. Evdokimov, N. M.; Magedov, I. V.; Kireev, A. S.; Kornienko, A. One-step, three-component synthesis of pyridines and 1,4-dihydropyridines with manifold medicinal utility. *Org. Lett.* **2006**, *8*, 899-902.
49. Eissa, A. M. F.; Ezz El-Arab, E. M.; Farag, A. M.; Moharram, H. H. Synthesis and biological evaluation of pyrido[2,3.d]pyrimidine as antitumor effect. *Egyptian J. Chem.* **2006**, *49*, 761-774.
50. Brandt, W.; Mologni, L.; Preu, L.; Lemcke, T.; Gambacorti-Passerini, C.; Kunick, C. Inhibitors of the RET tyrosine based on a 2-(alkylsulfanyl)-4-(3-thienyl)nicotinonitrile scaffold. *Eur. J. Med. Chem.* **2010**, *45*, 2919-2927.



51. Attaby, F.; Elghandour A. H. H.; Ali, M. A.; Ibrahim, Y. M. Synthesis, reactions, and antiviral activity of 6'-amino-2'-thioxo-1',2-dihydro-3,4'-bipyridine-3'-5'-dicarbonitrile. *Phosphorus, Sulfur and Silicon and the Related Elements* **2007**, *182*, 695-709.
52. Cabrerizo, M. A.; Soto, J. L. Synthesis of heterocycles. III. 2-Amino-3,5-dicyano-4-aryl-6-alkoxypyridines from benzylidenemalononitriles. *Anales de Quimica* **1974**, *70*, 951-958.
53. Basyouni, W. M. Synthesis of novel substituted [1,2,4]triazolo[1,5-a]pyridines and their related pyrano[2,3-d]imidazole derivatives. *Acta Chim. Slov.* **2003**, *50*, 223-238.
54. Dai, D.; Burgeson, J. R.; Tyavanagimatt, S. R.; Byrd, C. M.; Hruby, D. E. Thienopyridine Derivatives for the Treatment and Prevention of Dengue Virus Infections. US patent 0129677 (A1), May 23, 2013.
55. Taliani, S.; Bellandi, M.; La Motta, C.; Da Settimo, F. A<sub>3</sub> receptor ligands: past, present and future trends. *Curr. Topics Med. Chem.* **2010**, *10*, 942-975.
56. Glukhova, A.; Thal, D. M.; Nguyen, A. T.; Vecchio, E. A.; Jorg, M.; Scammells, P. J.; May, L. T.; Sexton, P. M.; Christopoulos, A. Structure of the adenosine A<sub>1</sub> receptor reveals the basis for subtype selectivity. *Cell* **2017**, *168*, 867-877.e13.
57. Molecular Operating Environment; C.C.G., I., 1255 University St., Suite 1600, Montreal, Quebec, Canada, H3B 3X3.
58. Jones, G.; Willett, P.; Glen, R. C.; Leach, A. R.; Taylor, R. Development and validation of a genetic algorithm for flexible docking. *J. Mol. Biol.* **1997**, *267*, 727-748.
59. Morris, G. M.; Goodsell, D. S.; Halliday, R. S.; Huey, R.; Hart, W. E.; Belew, R. K.; Olson, A. J. Automated docking using a Lamarckian genetic algorithm and an empirical binding free energy function. *J. Comput. Chem.* **1998**, *19*, 1639-1662.
60. Morris, G. M.; Huey, R.; Lindstrom, W.; Sanner, M. F.; Belew, R. K.; Goodsell, D. S.; Olson, A. J. AutoDock4 and AutoDockTools4: Automated docking with selective receptor flexibility. *J. Comput. Chem.* **2009**, *30*, 2785-2791.

61. Dallakyan, S.; Olson, A. J. Small-molecule library screening by docking with PyRx. *Methods Mol. Biol.* **2015**, *1263*, 243-250.
62. Liu, W.; Chun, E.; Thompson, A. A.; Chubukov, P.; Xu, F.; Katritch, V.; Han, G. W.; Roth, C. B.; Heitman, L. H.; IJzerman, A. P.; Cherezov, V.; Stevens, R. C. Structural basis for allosteric regulation of GPCRs by sodium ions. *Science* **2012**, *337*, 232-236.
63. Dal Ben, D.; Buccioni, M.; Lambertucci, C.; Marucci, G.; Santinelli, C.; Spinaci, A.; Thomas, A.; Volpini, R. Simulation and comparative analysis of different binding modes of non-nucleoside agonists at the A<sub>2A</sub> adenosine receptor. *Mol. Inform.* **2016**, *35*, 403-413.
64. Rodriguez, D.; Gao, Z. G.; Moss, S. M.; Jacobson, K. A.; Carlsson, J. Molecular docking screening using agonist-bound GPCR structures: probing the A<sub>2A</sub> adenosine receptor. *J. Chem. Inf. Model* **2015**, *55*, 550-563.
65. Dal Ben, D.; Buccioni, M.; Lambertucci, C.; Marucci, G.; Thomas, A.; Volpini, R.; Cristalli, G. Molecular modeling study on potent and selective adenosine A<sub>3</sub> receptor agonists. *Bioorg. Med. Chem.* **2010**, *18*, 7923-7930.
66. Congreve, M.; Andrews, S. P.; Dore, A. S.; Hollenstein, K.; Hurrell, E.; Langmead, C. J.; Mason, J. S.; Ng, I. W.; Tehan, B.; Zhukov, A.; Weir, M.; Marshall, F. H. Discovery of 1,2,4-triazine derivatives as adenosine A<sub>2A</sub> antagonists using structure based drug design. *J. Med. Chem.* **2012**, *55*, 1898-1903.
67. Lebon, G.; Warne, T.; Edwards, P. C.; Bennett, K.; Langmead, C. J.; Leslie, A. G.; Tate, C. G. Agonist-bound adenosine A<sub>2A</sub> receptor structures reveal common features of GPCR activation. *Nature* **2011**, *474*, 521-525.
68. Di Cesare Mannelli, L.; Lucarini, E.; Micheli, L.; Mosca, I.; Ambrosino, P.; Soldovieri, M.V.; Martelli, A.; Testai, L.; Taglialatela, M.; Calderone, V.; Ghelardini, C. Effects of natural and synthetic isothiocyanate-based H<sub>2</sub>S-releasers against chemotherapy-induced neuropathic pain: Role of Kv7 potassium channels. *Neuropharmacology* **2017**, *121*, 49-59.

69. Ribeiro, J. A.; Sebastião, A.M. Caffeine and adenosine. *J. Alzheimer Dis.* **2010**, *20* (Suppl 1), S3-15.
70. Górská, A.M.; Gołembiowska, K. The role of adenosine A<sub>1</sub> and A<sub>2A</sub> receptors in the caffeine effect on MDMA-induced DA and 5-HT release in the mouse striatum. *Neurotox. Res.* **2015**, *27*, 229-245.
71. Maltese, M.; Martella, G.; Imbriani, P.; Schuermans, J.; Billion, K.; Sciamanna, G.; Farook, F.; Ponterio, G.; Tassone, A.; Santoro, M.; Bonsi, P.; Pisani, A.; Goodchild, R.E. Abnormal striatal plasticity in a DYT11/SGCE myoclonus dystonia mouse model is reversed by adenosine A<sub>2A</sub> receptor inhibition. *Neurobiol. Dis.* **2017**, *108*, 128-139.
72. Bartolini, A.; Di Cesare Mannelli, L.; Ghelardini, C. Analgesic and antineuropathic drugs acting through central cholinergic mechanisms. *Recent Pat. CNS Drug Discov.* **2011**, *6*, 119-140.
73. Ghelardini, C.; Galeotti, N.; Bartolini, A. Caffeine induces central cholinergic analgesia. *Naunyn Schmiedebergs Arch. Pharmacol.* **1997**, *356*, 590-595.
74. Di Cesare Mannelli, L.; Ghelardini, C.; Calvani, M.; Nicolai, R.; Mosconi, L.; Toscano, A.; Pacini, A.; Bartolini, A. Neuroprotective effects of acetyl-L-carnitine on neuropathic pain and apoptosis: a role for the nicotinic receptor. *J Neurosci Res.* **2009**, *87*, 200-207.
75. Di Cesare Mannelli, L.; Pacini, A.; Matera, C.; Zanardelli, M.; Mello, T.; De Amici, M.; Dallanocce, C.; Ghelardini, C. Involvement of  $\alpha 7$  nAChR subtype in rat oxaliplatin-induced neuropathy: effects of selective activation. *Neuropharmacology* **2014**, *79*, 37-48.
76. Vincenzi, F.; Targa, M.; Romagnoli, R.; Merighi, S.; Gessi, S.; Baraldi, P.G.; Borea, P.A.; Varani, K. TRR469, a potent A<sub>1</sub> adenosine receptor allosteric modulator, exhibits anti-nociceptive properties in acute and neuropathic pain models in mice. *Neuropharmacology* **2014**, *81*, 6-14.
77. Varani, K.; Massara, A.; Vincenzi, F.; Tosi, A.; Padovan, M.; Trotta, F.; Borea, P.A. Normalization of A<sub>2A</sub> and A<sub>3</sub> adenosine receptor up-regulation in rheumatoid arthritis patients by treatment with anti-tumor necrosis factor alpha but not methotrexate. *Arthritis Rheum.* **2009**, *60*, 2880-2891.

78. Varani, K.; Merighi, S.; Gessi, S.; Klotz, K.-N.; Leung, E.; Baraldi, P.G.; Cacciari, B.; Romagnoli, R.; Spalluto, G.; Borea, P.A. [<sup>3</sup>H]MRE 3008F20: a novel antagonist radioligand for the pharmacological and biochemical characterization of human A<sub>3</sub> adenosine receptors, *Mol. Pharmacol.* **2000**, *57*, 968-975.
79. Ravani, A.; Vincenzi, F.; Bortoluzzi, A.; Padovan, M.; Pasquini, S.; Gessi, S.; Merighi, S.; Borea, P.A.; Govoni, M.; Varani, K. Role and function of A<sub>2A</sub> and A<sub>3</sub> adenosine receptors in patients with ankylosing spondylitis, psoriatic arthritis and rheumatoid arthritis. *Int. J. Mol. Sci.* **2017**, *18*, 697.
80. McGrath, J.C.; Lilley, E. Implementing guidelines on reporting research using animals (ARRIVE etc.): new requirements for publication in BJP. *Br. J. Pharmacol.* **2015**, *172*, 3189-3193.
81. Cavaletti, G.L.; Tredici, G.; Petruccioli, M.G.; Dondé, E.; Tredici, P.; Marmioli, P.; Minoia, C.; Ronchi, A.; Bayssas, M.; Etienne, G.G. Effects of different schedules of oxaliplatin treatment on the peripheral nervous system of the rat. *Eur. J. Cancer* **2001**, *37*, 2457-2463.
82. Di Cesare Mannelli, L.; Pacini, A.; Bonaccini, L.; Zanardelli, M.; Mello, T.; Ghelardini C. Morphologic features and glial activation in rat oxaliplatin-dependent neuropathic pain. *J Pain.* **2013**, *14*, 1585-1600.
83. Stewart, J. J. MOPAC: a semiempirical molecular orbital program. *J. Comput. Aided Mol. Des.* **1990**, *4*, 1-105.
84. ICH Q2B, Validation of Analytical Procedure: Methodology, International Conference on Harmonisation of Technical Requirements for Registration of Pharmaceuticals for Human Use, 1996. <http://www.ich.org/products/guidelines/quality/article/quality-guidelines.html>, (accessed Nov 6, 1996).

**Figure Captions.****Chart 1.**

Previously and currently reported amino-3,5-dicyanopyridines as AR ligands.

**Figure 1.** Competition curves of specific [<sup>3</sup>H]-DPCPX binding to hA<sub>1</sub>ARs of compounds **9-12** (A). Increase of forskolin-stimulated cAMP levels in hA<sub>1</sub>AR CHO cells by compounds **9-12** relative to the effect of DPCPX set at 100% (B). Data represent means ± SEM of four experiments each performed in triplicate.

**Figure 2. A.** Docking conformations of the synthesized compounds at the hA<sub>1</sub>AR (PDB: 5UEN<sup>56</sup>) cavity, taking **9** as template. Key receptor amino acids are indicated. **B.** Schematic view of the compound-receptor interaction (developed with the Ligand Interaction tool within MOE).

**Figure 3.** Top-view of the docking conformations of the synthesized compounds at the hA<sub>1</sub>AR (PDB: 5UEN<sup>56</sup>) binding site, taking **9** as example: detailed view of the interactions between the 6-substituent and the receptor aminoacids at the entrance of the binding cavity.

**Figure 4. A-B.** Ligand-target interaction energies calculated with the *IF-E 6.0* tool within MOE (see text for details) for sets of compounds differing only based on the 4-substituent. The receptor's amino acids located close to the 4-substituent were considered and are displayed in panel C. Data are represented as kcal mol<sup>-1</sup>. The results show a significant interaction with Thr277<sup>7,42</sup> for residues presenting a polar atom at the 3-endocyclic position within the 4-substituent (i.e. **19** and **26** in the first set and **18** and **24** in the second set). **C.** Detail of the ligand-target interaction at the 4-substituent (compound **26** is shown in this figure). The key residues (PDB: 5UEN<sup>56</sup>) involved in this interaction are displayed and indicated.

**Figure 5.** **A.** Docking conformations of the synthesized compounds at the hA<sub>2A</sub>AR cavity, taking compound **9** (green) as template. Key receptor amino acids are indicated. The position of the 4-heterocycle corresponds to the one of the 2-chlorophenol substituent of the 3-amino-1,2,4-triazine derivative (red) co-crystallized with the hA<sub>2A</sub>AR (pdb code: 3UZC<sup>66</sup>). **B.** Top-view of the docking conformations of the synthesized compounds at the A<sub>1</sub>AR cavity, taking compound **9** as example: detailed view of the interaction between the 6-substituent and the receptor aminoacids at the entrance of the binding cavity. **C.** Binding mode of compound **17** at the hA<sub>3</sub>AR cavity, analogue to the top-score docking conformations at the hA<sub>1</sub>AR and hA<sub>2A</sub>AR. Key receptor residues are indicated. This binding mode was observed only for some of the analyzed derivatives at the hA<sub>3</sub>AR cavity.

**Figure 6.** Effects of selected compounds against neuropathic pain in mice. Neuropathy was induced by repeated i.p. injection of oxaliplatin (2.4 mg kg<sup>-1</sup>, daily). The hypersensitivity to a cold thermal stimulus was measured on day 15 by the Cold plate test (latency to pain related behaviors as paw lifting or licking). Compounds **9-12** were administered p.o, measurements were performed 15, 30, 45, and 60 min after. Control mice were treated with vehicle. Each value represents the mean of 10 mice per group, performed in 2 different experimental sets. \*\*P < 0.01 vs vehicle + vehicle treated mice. ^P < 0.05 and ^^P < 0.01 vs oxaliplatin + vehicle treated mice.

**Figure 7.** Effects of caffeine against neuropathic pain in mice. Role of nAChRs. Neuropathy was induced by repeated i.p. injection of oxaliplatin (2.4 mg kg<sup>-1</sup>, daily). The hypersensitivity to a cold thermal stimulus was measured on day 15 by the Cold plate test (latency to pain related behaviors as paw lifting or licking). Caffeine was administered p.o. at 10 mg kg<sup>-1</sup>. The non-selective nAChR antagonist mecamylamine (meca; 2 mg kg<sup>-1</sup> i.p.) and the selective alpha7 nAChR antagonist methyllycaconitine (MLA; 6 mg kg<sup>-1</sup> i.p.) were administered 15 min before caffeine. Measurements were performed overtime after the injection of caffeine or vehicle (in control mice). Values are reported as mean of 10 mice per group (two different experimental sets). \*\*P < 0.01 vs vehicle +

vehicle treated mice.  $^{\wedge}P < 0.05$  and  $^{\wedge\wedge}P < 0.01$  vs oxaliplatin + vehicle treated mice.  $^{\circ}P < 0.01$  vs oxaliplatin + caffeine treated mice.

**Figure 8.** Effects of nicotinic antagonisms on compound **9** anti-hyperalgesic efficacy. Neuropathy was induced by repeated i.p. injection of oxaliplatin (2.4 mg kg<sup>-1</sup>, daily). The hypersensitivity to a cold thermal stimulus was measured on day 15 by the Cold plate test (latency to pain related behaviors as paw lifting or licking). The non-selective nAChR antagonist mecamylamine (meca; 2 mg kg<sup>-1</sup> i.p.) and the selective  $\alpha 7$  nAChR antagonist methyllycaconitine (MLA; 6 mg kg<sup>-1</sup> i.p.) were administered 15 min before **9** (0.3 mg kg<sup>-1</sup> p.o.). Measurements were performed overtime after the injection of **9** or vehicle (in control mice). Values are reported as mean of 10 mice per group (two different experimental sets).  $^{**}P < 0.01$  vs vehicle + vehicle treated mice.  $^{\wedge}P < 0.05$  and  $^{\wedge\wedge}P < 0.01$  vs oxaliplatin + vehicle treated mice.  $^{\circ}P < 0.01$  vs oxaliplatin + **9** treated mice.

**Figure 9.** Effects of nicotinic antagonisms on **10** anti-hyperalgesic efficacy. Neuropathy was induced by repeated i.p. injection of oxaliplatin (2.4 mg kg<sup>-1</sup>, daily). The hypersensitivity to a cold thermal stimulus was measured on day 15 by the Cold plate test (latency to pain related behaviors as paw lifting or licking). The non-selective nAChR antagonist mecamylamine (meca; 2 mg kg<sup>-1</sup> i.p.) and the selective  $\alpha 7$  nAChR antagonist methyllycaconitine (MLA; 6 mg kg<sup>-1</sup> i.p.) were administered 15 min before **10** (0.3 mg kg<sup>-1</sup> p.o.). Measurements were performed overtime after the injection of **10** or vehicle (in control mice). Values are reported as mean of 10 mice per group (two different experimental sets).  $^{**}P < 0.01$  vs vehicle + vehicle treated mice.  $^{\wedge}P < 0.05$  and  $^{\wedge\wedge}P < 0.01$  vs oxaliplatin + vehicle treated mice.  $^{\circ}P < 0.01$  vs oxaliplatin + **10** treated mice.

**Scheme 1.**

**Reagents and conditions.** a) Malononitrile, thiophenol, TBAF, H<sub>2</sub>O, 80 °C; b) Na<sub>2</sub>S, anhydrous DMF, 80 °C; 1N HCl, rt; c) R<sup>3</sup>CH<sub>2</sub>Br, NaHCO<sub>3</sub>, anhydrous DMF, rt; d) NH<sub>2</sub>COCH<sub>2</sub>Cl, 10% KOH, DMF, rt (compound **5**); e) NH<sub>2</sub>CH<sub>2</sub>CH<sub>2</sub>OH, DMF, 100 °C; (for R<sup>3</sup> substituent details see Table 1).

**Scheme 2.**

**Reagents and conditions.** a) malononitrile, NaOCH<sub>3</sub>, TBAF, MeOH, reflux; b) 12N HCl, glacial AcOH, 100 °C; c) BrCH<sub>2</sub>CH<sub>2</sub>OH, NaHCO<sub>3</sub>, anhydrous DMF, 80 °C, microwave irradiation.

**Scheme 3.**

**Reagents and conditions.** a) isoamyl nitrite, CuCl<sub>2</sub>, CH<sub>3</sub>CN, rt; b) R<sup>1</sup>-NH<sub>2</sub>, anhydrous DMF, rt.

**Scheme 4.**

**Reagents and conditions.** a) acetic anhydride, pyridine, reflux; b) Na<sub>2</sub>S, anhydrous DMF, 50 °C; 1N HCl, rt; c) BrCH<sub>2</sub>CH<sub>2</sub>OH, NaHCO<sub>3</sub>, anhydrous DMF, rt.



Table of Contents Graphic

